
Adaptive Reinforcement Learning for Unobservable Random Delays

John Wikman

EECS and Digital Futures
KTH Royal Institute of Technology
Stockholm, Sweden
jwikman@kth.se

Alexandre Proutiere

EECS and Digital Futures
KTH Royal Institute of Technology
Stockholm, Sweden
jwikman@kth.se

David Broman

EECS and Digital Futures
KTH Royal Institute of Technology
Stockholm, Sweden
dbro@kth.se

Abstract

In standard Reinforcement Learning (RL) settings, the interaction between the agent and the environment is typically modeled as a Markov Decision Process (MDP), which assumes that the agent observes the system state instantaneously, selects an action without delay, and executes it immediately. In real-world dynamic environments, such as cyber-physical systems, this assumption often breaks down due to delays in the interaction between the agent and the system. These delays can vary stochastically over time and are typically *unobservable*, meaning they are unknown when deciding on an action. Existing methods deal with this uncertainty conservatively by assuming a known fixed upper bound on the delay, even if the delay is often much lower. In this work, we introduce the *interaction layer*, a general framework that enables agents to adaptively and seamlessly handle unobservable and time-varying delays. Specifically, the agent generates a matrix of possible future actions to handle both unpredictable delays and lost action packets sent over networks. Building on this framework, we develop a model-based algorithm, *Actor-Critic with Delay Adaptation (ACDA)*, which dynamically adjusts to delay patterns. Our method significantly outperforms state-of-the-art approaches across a wide range of locomotion benchmark environments.

1 Introduction

State-of-the-art reinforcement learning (RL) algorithms, such as Proximal Policy Optimization (PPO) [1] and Soft Actor-Critic (SAC) [2], are typically built on the assumption that the environment can be modeled as a Markov Decision Process (MDP). This framework implicitly assumes that the agent observes the current state instantaneously, selects an action without delay, and executes it immediately.

However, this assumption often breaks down in real-world systems due to *interaction* delays. These delays arise from various sources: the time taken for sensors to collect and transmit observations, the computation time needed for the agent to select an action, and the transmission and actuation delay when executing that action in the environment (as illustrated in Figure 1). Delays pose no issue if the state of the environment is not evolving between its observation and the execution of the selected action. But in continuously evolving systems—such as robots operating in the physical

world—the environment’s state may have changed by the time the action is executed [3]. Delays have been recognized as a key concern when applying RL to cyber-physical systems [4]. Outside the scope of RL, delays have also been studied in classic control [5, 6].

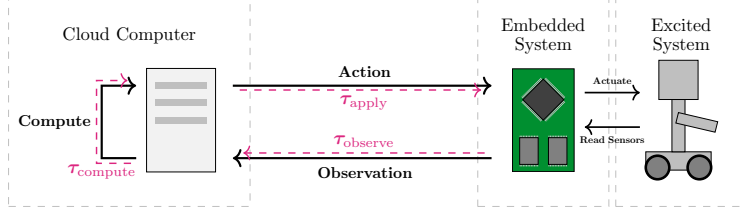


Figure 1: Illustration of a setup affected by interaction delays. Any delay between the embedded system and the excited system is considered negligible or otherwise accounted for. The factors contributing to interaction delay are τ_{observe} (τ_o), τ_{compute} (τ_c), and τ_{apply} (τ_a). See Section 3.1 for more details about these factors.

These interaction delays can be implicitly modeled by altering the transition dynamics of the MDP to form a partially observable Markov decision process (POMDP), in which the agent only receives outdated sensor observations. While this approach is practical and straightforward, it limits the agent’s access to information about the environment’s evolution during the delay period.

Another common approach to handling delays in RL is to enforce that actions are executed after a fixed delay [7, 8, 9, 10, 11, 12, 13]. This is typically implemented by introducing an action buffer between the agent and the environment, ensuring that all actions are executed after a predefined delay. However, this method requires prior knowledge of the maximum possible delay and enforces that all actions incur this worst-case delay—even when most interactions in practice experience minimal or no delay. The advantage of this fixed-delay approach is that it provides the agent with perfect information about when its actions will take effect, simplifying decision-making. However, it is overly conservative and fails to adapt and account for variability in delay. Note that state-of-the-art algorithms for delayed MDPs, such as BPQL [14] and VDPO [15], rely on this fixed-delay paradigm.

Moving beyond this fixed-delay framework is challenging, especially because in real-world systems, delays are often unobservable. The agent does not know, at decision time, how long it will take for an action to be executed. One existing approach that attempts to address varying delays is DCAC [16], but it assumes perfect knowledge of the delay for each action at the time it is chosen. This assumption is rarely practical.

In this paper, we make the following contributions:

(i) We introduce a novel framework, the *interaction layer*, which allows agents to adapt to randomly varying delays—even when these delays are unobservable. In this setup, the agent generates a matrix of candidate actions ahead of time, each intended for a possible future execution time. Specifically, the design handles both (a) that the future actions can have varying delays, and (b) that action packets sent over a network can be lost or arrive in incorrect order. The actual action is selected at the interaction layer once the delay is revealed. This approach enables informed decision-making under uncertainty and robust behavior in the presence of stochastic, unobservable delays (Section 3).

(ii) We develop a new model-based reinforcement learning algorithm, *Actor-Critic with Delay Adaptation (ACDA)*, which leverages the interaction layer to adapt dynamically to varying delays. The algorithm provides two key concepts: (a) instead of using states as input to the policy, it uses a distribution of states as an embedding that enables the generation of more accurate time series of actions, and (b) an efficient heuristic to determine which of the previously generated actions are executed. These actions are needed to compute the state distributions. The approach is particularly efficient when delays are temporally correlated, something often seen in scenarios when communicating over transmission channels (Section 4).

(iii) We evaluate ACDA on a suite of MuJoCo locomotion tasks from the Gymnasium library [17], using randomly sampled delay processes designed to mimic real-world latency sources. Our results show that ACDA, equipped with the interaction layer, consistently outperforms state-of-the-art algorithms designed for fixed delays. It achieves higher average returns across all benchmarks except

one, where its performance remains within the standard deviation of the best constant-delay method (Section 5).

2 Related Work

To our knowledge, there is no previous work that explicitly allows for agents to make informed decisions under random unobservable delays in RL.

Much of existing work on how to handle delays in RL acts as if delays are constant equal to h , in which case, the problem can be modeled as an MDP with augmented state $(s_t, a_t, a_{t+1}, \dots, a_{t+h-1})$ consisting of the last observed state and memorized actions to be applied in the future [18]. Even if the true delay is not constant, a construction used in previous work is to enforce constant interaction delay through *action buffering*, under the assumption that the maximum delay does not exceed h time-steps.

By maintaining an action buffer that includes future actions to be applied, one may in principle use existing RL techniques to deal with constant delays. However, directly learning policies on augmented states is hard in practice, which has prompted the development of algorithms that make use of the delayed dynamics. The real-time actor-critic by Ramstedt and Pal [9] leverages the augmented state to optimize for a constant delay of one time step. A planning-based approach, called delay-aware trajectory sampling and proposed by Chen et al. [10], uses probabilistic ensemble with trajectory sampling [19] to plan further into the future using memorized actions from the augmented state together with a learned dynamics model. Earlier work by Firoiu, Ju, and Tenenbaum [8] learned a model of the dynamics to perform state-rollouts to use as input for the policy. Recently, Wang et al. [20] looked at variations in model structures, both for policy and critic inputs.

Recent work by Kim et al. [14] describes belief projection-based Q-learning (BPQL) that explicitly uses the delayed dynamics under constant delay to simplify the critic learning. This work shows the ability to achieve good performance during evaluation over longer delays, despite a simple structure of the learned functions. Our algorithm in Section 4.3 use the same critic simplification, but applied to the randomly delayed setting.

Another approach explored for constant-delay RL is that of having delayed agent trying imitate an undelayed expert, which is employed in algorithms such as DIDA [11] and VDPO [15]. These assume access to the undelayed MDP, which in the real-world can be applied in sim-to-real scenarios, but not when training directly on the real physical system.

Work by Bouteiller et al. [16] also uses action buffering to reason about random delays, but assumes that delays are observable at the time when actions are being generated. In contrast, our work does not depend on such a strong assumption, i.e., we only require that delays are available in hindsight for actions that were applied to the underlying system (see Section 3.1).¹

One method of making informed decisions is to use a learned dynamics model of the system, for example to plan into future horizons or to estimate future states as policy inputs [7]. A commonly used dynamics model architecture is the recurrent state space model (RSSM) [21] that combine recurrent latent state with stochastically sampled states as inputs when transitioning in latent space. RSSM is designed to be used for planning algorithms, but can also be used for state prediction. The model used by Firoiu, Ju, and Tenenbaum [8] is similar to RSSM, but uses deterministic output of states from latent representation. Another approach using RSSM is DREAMER [22] which learns a latent state representation for the agent to make decisions in, but in an undelayed setting.

Our approach also learns a model to make decisions in latent space but does not follow the RSSM structure. Instead, our model (introduced in Section 4.2) follows a simpler structure that learns a latent representation describing an actual distribution over states rather than uncertainty about an assumed existing true state. By the definitions of [23], our model classifies as a multi-step prediction model with state abstraction, even though we are only estimating distributions.

¹We never observe the delay for generated actions that did not end up being applied to the system. Although it is possible to consider a real-world setup where you can collect this information as well, we do not need it for our algorithm in Section 4.

3 The Interaction Layer

In this section, we explain how random and unpredictable delays may affect the interaction between the agent and the system. To handle these delays, we introduce a new framework, called the *interaction layer* (Section 3.2), and model the way the agent and the system interact by a Partially Observable MDP (Section 3.3).

3.1 Delayed Markov decision processes

We consider a controlled dynamical system modeled as an MDP $\mathcal{M} = (S, A, p, r, \mu)$, where S and A are the state and action spaces, respectively, where $p(s'|s, a)_{(s', s, a) \in S \times S \times A}$ represents the system dynamics in the absence of delays, r is the reward function, and μ is the distribution of the initial state.

As in usual MDPs, we assume that at the beginning of each step t , the state of the system is sampled, but this information does not reach the agent immediately, but after an observation delay, τ_o . After the agent receives the information, an additional computational delay, τ_c , occurs due to processing the information and deciding on an appropriate action. The action created by agent is then communicated to the system, with an additional final delay τ_a before this action can be applied to the system. The delays² (τ_o, τ_c, τ_a) are random variables that may differ across steps and can be correlated. These delays are unobservable to the agent.

3.2 Handling delays via the interaction layer

The unpredictable delays pose significant challenges from the agent’s perspective. First, the agent cannot respond immediately to the newly observed system state at each step. Second, the agent cannot determine when the selected action will be applied to the system. To address these issues, we introduce the *interaction layer*, consisting of an *observer* and of an *action buffer*, as illustrated in Figure 2. The interaction layer is a direct part of the system that performs sensing and actuation, whereas the agent can be far away, communicating over a network. Within the interaction layer, the observer is responsible for sampling the system’s state and sending relevant information to the agent. The agent generates a matrix of possible actions. These are sent back to the interaction layer and stored in the action buffer. Depending on when the actions arrive in the action buffer, it selects a row of actions, which are then executed in the following steps if no further decision is received. The rest of this section gives technical details of the interaction layer, whereas Section 4 details the policy for generating actions at the agent.

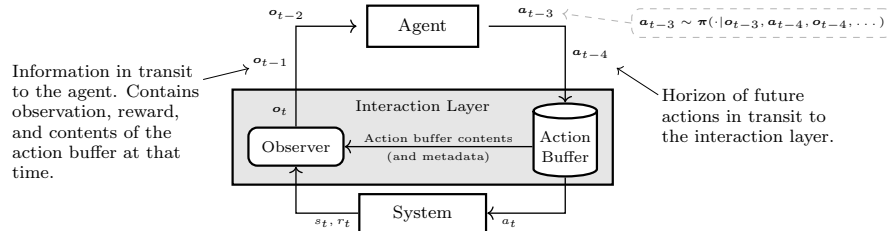


Figure 2: Illustration of the interaction layer and how the agent interacts with it from a global perspective. As the observation is received from the dynamical system, the next action is immediately applied from the action buffer. Packets in transit with random delay imply partial observability.

Action packet. After that the agent receives an observation packet o_t (generated at step t by the interaction layer, described further below), the agent generates and sends an action packet a_t . The

²We assume that The total delay $\tau_o + \tau_c + \tau_a$ is measured in number of steps. In Appendix F.1, we present a similar model where delays can take any real positive value.

packet includes time stamp t , and a matrix of actions, as follows:

$$\mathbf{a}_t = \left(t, \begin{bmatrix} a_1^{t+1} & a_2^{t+1} & a_3^{t+1} & \dots & a_h^{t+1} \\ a_1^{t+2} & a_2^{t+2} & a_3^{t+2} & \dots & a_h^{t+2} \\ \vdots & \vdots & \vdots & \ddots & \vdots \\ a_1^{t+L} & a_2^{t+L} & a_3^{t+L} & \dots & a_h^{t+L} \end{bmatrix} \right). \quad (1)$$

The i -th row of the matrix of the action packet corresponds to the sequence of actions that would constitute the action buffer if the packet reaches the interaction layer at time $t + i$. The reason for using a matrix instead of a vector is that subsequent columns specify which actions to take if a new action packet does not arrive at the interaction layer at a specific time step. For instance, if an action packet arrives at time $t + 2$, then the interaction layer uses the first action in the buffer (a_1^{t+2} in this case). That is, the first column is always used when a new packet arrives at each time step. If no packet arrives for a specific time step, the other columns are used instead (as explained more below in the description of the action buffer). This approach enables adaptivity for the agent: it can generate actions for specific delays without knowing what the delay is going to be ahead of time. Figure 3 illustrates when an action packet arrives at the interaction layer and a row is inserted into the action buffer (3rd row in this case because the packet arrived with a delay of 3).

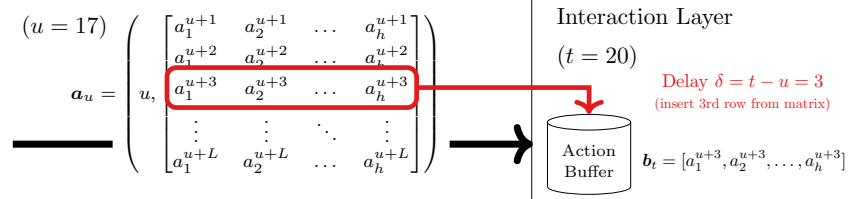


Figure 3: Example: Suppose an action packet timestamped by the agent with time $u = 17$, \mathbf{a}_u , arrives at the action layer at time 20. Then, at time $t = 20$, $\delta_{20} = 3$, and $c_{20} = 0$. Now, suppose that 2 time units elapse without any new action packet arriving. Then, at time $t = 22$, $\delta_{22} = 3$ and counter $c_{22} = 2$. Hence, equation $t = u + \delta_{22} + c_{22} = 17 + 3 + 2 = 22$ holds.

Action buffer. The action buffer is responsible for executing an action each time step. If no new action arrives at a time step, the next item in the buffer is used. At the beginning of step t , the action buffer contains the following information: \mathbf{b}_t , a sequence of h actions to be executed next, and δ_t , the delay of the action packet from which the actions \mathbf{b}_t were taken from. For instance, if an action packet \mathbf{a}_u arrives at the action buffer at time t , then $\delta_t = t - u$, where u is the time stamp of the action packet \mathbf{a}_u that the agent created. If instead no new action packet arrived at time t , then $\delta_t = \delta_{t-1}$. To enable the use of an appropriate action even if no new packet arrives at a specific time step, the content of the buffer is shifted one step forward, as shown in Figure 4. Finally, the action buffer includes a counter c_t that records how many steps have passed since the action buffer was updated. The following invariant always holds: $t = u + \delta_t + c_t$. For a concrete example, see the caption of Figure 3.

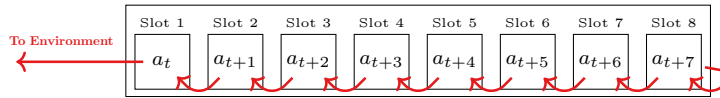


Figure 4: Action buffer shifting actions. Final slot is repeated. (Example: horizon $h = 8$)

Observation packet. The observer builds an observation packet \mathbf{o}_t at the beginning of step t . To this aim, it samples the system state s_t , collects information \mathbf{b}_t , δ_t , c_t about the action buffer, forms the observation packet $\mathbf{o}_t = (t, s_t, \mathbf{b}_t, \delta_t, c_t)$, and sends it to the agent.

Enhancing the information contained in the observation and action packets (compared to the undelayed MDP scenario) allows the agent to make more informed decisions and ensures the system does not run out of actions when action packets experience delays. However, this is insufficient to model our delayed system as an MDP. This is because the agent does not have the knowledge of all the observation and action packets currently in transit. Therefore, we use the formalism of a POMDP to accurately describe the system dynamics.

3.3 The POMDP model

Next, we complete the description of our delayed MDP and model it as a POMDP. To this aim, we remark that the system essentially behaves as if in each step t , the agent immediately observes \mathbf{o}_t and selects an action packet \mathbf{a}_t that arrives at the interaction layer d_t steps after the observation \mathbf{o}_t was made, where $d_t > 0^3$. We assume that d_t is generated according to some distribution D^4 . Furthermore, we assume that observation packets \mathbf{o}_t arrive in order at the agent. In this framework—where the agent selects an action packet \mathbf{a}_t as soon as the observation \mathbf{o}_t is generated—the single delay d_t replaces the three delays (τ_o, τ_c, τ_a) .

The time step t is a local time tag from the perspective of the interaction layer. Our POMDP formulation does not assume a synchronized clock between the agent and the interaction layer. The agent acts asynchronously and generates an action packet upon receiving an observation packet.

We define \mathcal{I}_t as the set of action packets in transit at the beginning of step t , along with the times at which these packets will arrive at the interaction layer (\mathcal{I}_t is a set containing items on the form $(u + d_u, \mathbf{a}_u)$). In reality, delays are observed only when action packets reach the interaction layer, and the agent does not necessarily know whether the action packets already generated have reached the interaction layer. Hence we must assume that \mathcal{I}_t is not observable by the agent. The framework we just described corresponds to a POMDP, which we formalize in Appendix C in detail.

4 Actor-Critic with Delay Adaptation

This section introduces *actor-critic with delay adaptation* (ACDA), a model-based RL algorithm that uses the interaction layer to adapt on-the-fly to varying unobservable delays, contrasting to state-of-the-art methods that enforce a fixed worst-case delay. A challenge with varying unobservable delays is that the agent lacks perfect information about the actions to be applied in the future. Indeed, it does not know when recently sent actions will arrive at the interaction layer. ACDA solves this with a heuristic (Section 4.1) that is effective when delays are temporally correlated.

The actions selected by ACDA will vary in length depending on the delay that we are generating actions for. This lends itself poorly to commonly used policy function approximators in deep RL such as multi-layer perceptrons (MLPs), that assume a fixed size of input. ACDA solves this with a model-based distribution agent (Section 4.2) that embeds the variable length input into fixed size embedding of the distribution over the state to which the generated action will be applied. The fixed size embeddings are then used as input to an MLP to generate actions. ACDA learns a model of the environment dynamics online to compute these embeddings. Section 4.3 shows how we train ACDA.

4.1 Heuristic for Assumed Previous Actions

A problem with unobservable delays is that we do not know when our previously sent action packets will arrive at the interaction layer. This means that we do not know which actions that are going to be applied to the underlying system between generating the action packet and it arriving at the interaction layer. A naive assumption would be to assume the action buffer contents reported by the observation packet to be the actions that are going to be applied to the underlying system. However, this is unlikely to be true due to that the action buffer is going to be preempted by action packets already in transit.

ACDA employs a heuristic for estimating these previous actions to be applied to the system between \mathbf{o}_t being generated and \mathbf{a}_t arriving at the interaction layer. The heuristic assumes that, if \mathbf{a}_t arrives at time $t + k$ (it having delay k), then previous action packets will also have delay k . Such that \mathbf{a}_{t-1} will arrive at time $t + k - 1$, \mathbf{a}_{t-2} at $t + k - 2$, etc.

Under this assumption, a new action packet will preempt the action buffer at every single time step. This means that, if we assume a delay of k , the action applied to the underlying system will be the action in the first column of the k -th row in the action packet last received by the interaction layer.

³Note that d_t corresponds to the value δ_u if the action packet reaches the interaction layer at time u : $\delta_{t+d_t} = d_t$

⁴For simplicity, we assume that the delay process is markovian and independent of the contents of the action packets and the state of the interaction layer. However, our POMDP formalism can be extended to delay distributions that depend on the previous state, which is more general and realistic.

By memorizing the action packets previously sent, we can under this assumption select the actions that are going to be applied to the system as shown in Algorithm 1. When generating a_1^{t+k} , the first action on the k -th row in the action packet a_t , we use Algorithm 1 to determine the actions $(\hat{a}_1^{t+k}, \dots, \hat{a}_k^{t+k})$ that will be applied to the observed state s_t before a_1^{t+k} is executed. For the action a_2^{t+k} , we know that this is only going to be executed if no new action packet arrived at $t + k + 1$. We therefore extend the previous assumption and say that $(\hat{a}_1^{t+k}, \dots, \hat{a}_k^{t+k}, a_1^{t+k})$ are the actions applied to s_t before a_2^{t+k} is executed.

The main idea here is that the heuristic guesses the applied actions if the delay does not evolve too much over time. If the delay truly was constant, then all guesses would be accurate and ACDA would transform the POMDP problem to a constant-delay MDP. The heuristic’s accuracy is compromised during sudden changes in delay, such as network delay spikes. However, as we will see in the evaluation, occasional violations will not significantly impact overall performance.

Algorithm 1 Memorized Action Selection

Input $k \in \mathbb{Z}^+$ (Delay assumption)
 $a_{t-1}, a_{t-2}, \dots, a_{t-k}$ (Memorized Packets)

- 1: **for** $i \leftarrow 1$ to k **do**
- 2: $(t - i, M^{t-i}) = a_{t-i}$
- 3: \triangleright Unpacking action matrix M from packets
- 4: **return** $(\hat{a}_1^{t+k}, \dots, \hat{a}_k^{t+k}) = (M_{k,1}^{t-k}, \dots, M_{k,1}^{t-1})$

4.2 Model-Based Distribution Agent

The memorized actions used by ACDA are variable in length and therefore cannot be directly used as input to MLPs, unlike in constant-delay approaches. Instead, ACDA constructs an embedding z_1^{t+k} of the distribution $p(s_{t+k} | s_t, \hat{a}_1^{t+k}, \dots, \hat{a}_k^{t+k})$, where $\hat{a}_1^{t+k}, \dots, \hat{a}_k^{t+k}$ are the memorized actions. We then provide z_1^{t+k} as input to an MLP to generate a_1^{t+k} . This allows the policy to reason about the possible states in which the generated action will be executed. Note that we are only concerned with the distribution itself and never explicitly sample from it.

To compute these embeddings, we learn a model of the system dynamics using three components: EMBED_ω , STEP_ω , and EMIT_ω , where ω represents learnable parameters.

- $\hat{z}_0 = \text{EMBED}_\omega(s_t)$ embeds a state s_t into a distribution embedding \hat{z}_0 .
- $\hat{z}_{i+1} = \text{STEP}_\omega(\hat{z}_i, a_{t+i})$ updates the embedded distribution to consider what happens after also applying the action a_{t+i} . Such that if \hat{z}_i is an embedding of $p(s_{t+i} | s_t, a_t, \dots, a_{t+i})$, then \hat{z}_{i+1} is an embedding of $p(s_{t+i+1} | s_t, a_t, \dots, a_{t+i}, a_{t+i+1})$.
- The final component $\text{EMIT}_\omega(s_{t+i} | \hat{z}_i)$ allows for a state to be sampled from the embedded distribution. This component is not used when generating actions, and is instead only used during training to ensure that \hat{z}_i is a good embedding of $p(s_{t+i} | s_t, a_t, \dots, a_{t+i})$.

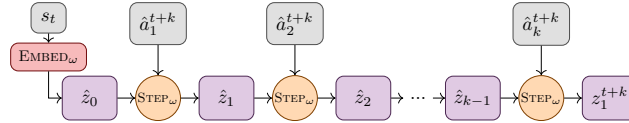


Figure 5: Illustration of the multi-step distribution model embedding $p(s_{t+k} | s_t, \hat{a}_1^{t+k}, \dots, \hat{a}_k^{t+k})$ as $\text{STEP}_\omega^k(\text{EMBED}_\omega(s_t), \hat{a}_1^{t+k}, \dots, \hat{a}_k^{t+k})$.

The way these components are used to produce the embedding z_1^{t+k} is illustrated in Figure 5. We use the notation $z_1^{t+k} = \hat{z}_k$ given that we are embedding the selected actions $(\hat{a}_1^{t+k}, \dots, \hat{a}_k^{t+k})$. We use the notation $\text{STEP}_\omega^k(\text{EMBED}_\omega(s_t), \hat{a}_1^{t+k}, \dots, \hat{a}_k^{t+k})$ to describe this multi-step embedding process. This notation is formalized in Appendix D.

The EMBED_ω and EMIT_ω components are implemented as MLPs, while STEP_ω is implemented as a gated recurrent unit (GRU). We provide detailed descriptions of these components in Appendix D. We learn these components online by collecting information from trajectories about observed states s_t and s_{t+n} and their interleaved actions $a_t, a_{t+1}, \dots, a_{t+n-1}$ in a replay buffer \mathcal{R} . The following loss function $\mathcal{L}(\omega)$ is used to minimize the KL-divergence between the model and the

underlying system dynamics: $\mathcal{L}(\omega) = \mathbb{E}_{(s_t, a_t, a_{t+1}, \dots, a_{t+n-1}, s_{t+n}) \sim \mathcal{R}} [-\log \text{EMIT}_\omega(s_{t+n} | z_n)]$ where $z_n = \text{STEP}_\omega^n(\text{EMBED}_\omega(s_t), a_t, a_{t+1}, \dots, a_{t+n-1})$.

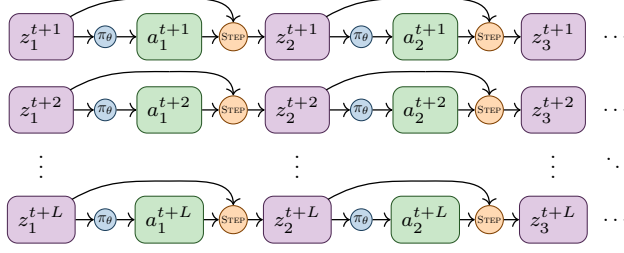


Figure 6: Generating the action packet from the embeddings. Each row in the figure corresponds to a row in the matrix of the action packet \mathbf{a}_t .

Given the embedding z_1^{t+k} , we produce a_1^{t+k} in the action packet \mathbf{a}_t using a policy $\pi_\theta(a_1^{t+k} | z_1^{t+k})$, i.e. generating actions given the (embedded) distribution over the state that the action will be applied to. This policy structure allows the agent to reason about uncertainties in future states when generating actions.

By extending the assumptions as shown in Section 4.1, we can also produce the embeddings z_2^{t+k} , z_3^{t+k} , etc., as illustrated in Figure 6. The complete process of constructing the action packet is formalized in Appendix D.

This model-based policy can also be applied in the constant-delay setting to achieve decent performance. We evaluate how this compares against a direct MLP function approximator in Appendix E.2, where we implement and evaluate the model-based policy in the BPQL algorithm.

4.3 Training Algorithm

This section describes the training procedure in Algorithm 2, used to optimize the parameters of the networks. It follows an actor-critic setup based on SAC. The training procedure of the critic Q_ϕ is similar to BPQL, where $Q_\phi(s, a)$ evaluate the value of actions a on undelayed system states s .

Algorithm 2 is split into three parts: trajectory sampling (L3-L12), transition reconstruction (L13), and training (L14-L15). We do this split to reduce the impact that the training procedure can have on the computational delay τ_c of the system. From the trajectory sampling we collect POMDP transition information $(\mathbf{o}_t, \mathbf{a}_t, r_t, \mathbf{o}_{t+1})$ where Γ_t is used to discern if s_t is in a terminal state.

An important aspect of Algorithm 2 is how trajectory information is reconstructed for training. Specifically, we reconstruct the trajectory $(s_0, a_0, r_0, s_1, a_1, \dots)$ from the perspective of the undelayed MDP, along with the policy input used to generate each action a_t . The policy input can be retrospectively recovered by examining the current action delay in the buffer (δ_t) and the number of times the buffer has shifted (c_t).

This trajectory reconstruction is necessary since we follow the BPQL algorithm’s actor-critic setup. The critic $Q_\phi(s_t, a_t)$ estimates values in the undelayed MDP, and we need to be able to regenerate actions a_t using the model-based policy to compute the TD-error. The details of trajectory reconstruction and the training algorithm is located in Appendix D.

Algorithm 2 Actor-Critic with Delay Adaptation

- 1: Init. policy π_θ , critic Q_ϕ , model ω , and replay \mathcal{R}
 - 2: **for** each epoch **do**
 - 3: Reset interaction layer state: $\mathbf{s}_0 \sim \mu, t = 0$
 - 4: Collected trajectory: $\mathcal{T} = \emptyset$
 - 5: Observe \mathbf{o}_0
 - 6: **while** terminal state not reached **do**
 - 7: **for** $k \leftarrow 1$ to L **do**
 - 8: Select $\hat{a}_1^{t+k}, \dots, \hat{a}_k^{t+k}$ by Alg. 1
 - 9: Create the k -th row of \mathbf{a}_t
 - 10: Send \mathbf{a}_t , observe $r_t, \mathbf{o}_{t+1}, \Gamma_{t+1}$
 - 11: Add $(\mathbf{o}_t, \mathbf{a}_t, r_t, \mathbf{o}_{t+1}, \Gamma_{t+1})$ to \mathcal{T}
 - 12: $t \leftarrow t + 1$
 - 13: Reconstruct transition info from \mathcal{T} , add to \mathcal{R}
 - 14: **for** $|\mathcal{T}|$ sampled batches from \mathcal{R} **do**
 - 15: Update π_θ, Q_ϕ and ω (by $\mathcal{L}(\omega)$)
-

5 Evaluation and Results

To assess the benefits of the interaction layer in a delayed setting, we simulate the POMDP described in Section 3.3, wrapping existing environments from the Gymnasium library [17] as the underlying system. Specifically, we aim to answer the question whether our ACDA algorithm that uses information from the interaction layer can outperform state-of-the-art algorithms under random delay processes.

We evaluate on the three delay processes shown in Figure 7. The first two delay processes $GE_{1,23}$ and $GE_{4,32}$ follow Gilbert-Elliot models [24, 25] where the delay alternate between good and bad states (e.g. a network or computational node being overloaded or having packets dropped). The third delay process MM1 is modeled after an M/M/1 queue [26] where sampled delay is the time spent in the queue by a network packet. The full definition of these delay processes are located in Appendix B.2. We expect that ACDA performs well under the Gilbert-Elliot processes that match the temporal assumptions of ACDA, whereas we expect ACDA to not perform as well with the M/M/1 queue delays that fluctuate more.

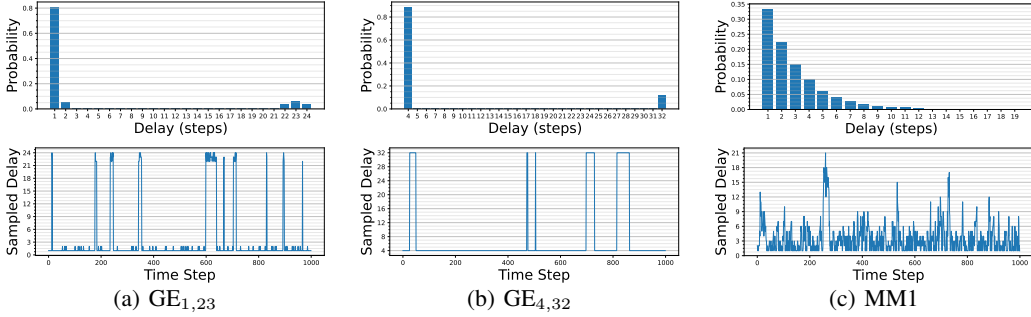


Figure 7: The delay processes we evaluate on, as a distribution histogram (above) and as a time series sampled delay over 1000 steps (below) for each delay process. See Appendix B.2 for their definitions.

The state-of-the-art algorithms we compare against are BPQL [14] and VDPO [15].⁵ As these are designed to operate under constant delay, we apply a *constant-delay augmentation* (CDA) to allow them to operate with constant delay in random delay processes. CDA converts the interaction layer POMDP into a constant-delay MDP by making agents act under the worst-case delay of a delay process.⁶ This augmentation process is described in Appendix A. In addition to the state-of-the-art algorithms, we also evaluate the performance of SAC, both with CDA and when it acts directly on the state from the observation packet (implicitly modeling delays). In Appendix E.3, we evaluate when CDA use an incorrect worst-case delay that holds most of the time, but is occasionally violated.

We evaluate average return over a training period of 1 million steps on MuJoCo environments in Gymnasium, following the procedure from related work in delayed RL. However, an issue with the MuJoCo environments is that they have deterministic transition dynamics, rendering them theoretically unaffected by delay. To better evaluate the effect of delay, we make the transitions stochastic by imposing a 5% noise on the actions. We motivate and specify this in Appendix B.1.

The average return is computed every 10000 steps by freezing the training weights and sampling 10 trajectories under the current policy. We report the best achieved average return—where the return is the sum of rewards over a trajectory—for each algorithm, environment, and delay process in Table 1. All achieved average returns are also presented in Appendix E.1 as time series plots together with tables showing the standard deviation.

⁵VDPO has an unfair advantage compared to BPQL and ACDA in that it has access to an undelayed copy of the underlying system. However, we leave this aspect of the VDPO algorithm unchanged since it does not outperform ACDA, or even BPQL in many benchmarks. We do not compare against DCAC as that is designed to operate under fully observable random delays, which is not the case in our problem setting.

⁶The MM1 delay process does not have a maximum delay. We use a reasonable worst-case of 16 steps.

Table 1: Best evaluated average return for each algorithm.

<i>Gymnasium env.</i>	Ant-v4			Humanoid-v4			HalfCheetah-v4			Hopper-v4			Walker2d-v4		
<i>Delay process</i>	GE _{1,23}	GE _{4,32}	MM1	GE _{1,23}	GE _{4,32}	MM1	GE _{1,23}	GE _{4,32}	MM1	GE _{1,23}	GE _{4,32}	MM1	GE _{1,23}	GE _{4,32}	MM1
SAC	14.22	-5.72	-0.58	862.18	494.43	921.04	2064.18	-158.78	20.69	306.91	279.74	333.06	708.33	60.86	604.80
SAC w/ CDA	69.28	18.93	102.00	414.05	230.45	613.03	128.47	591.32	550.84	426.92	315.47	627.59	428.44	257.18	2005.76
BPQL	2691.88	2509.52	3074.17	585.19	276.63	5435.29	4320.20	2136.36	4660.93	1328.71	433.29	3035.66	1215.91	875.09	3547.73
VDPO	2163.00	2266.99	2528.67	417.25	280.72	720.73	3144.23	3664.30	3831.96	709.20	330.44	1459.88	846.88	344.73	2144.25
ACDA	4112.78	2866.93	2898.46	4608.76	3725.59	5805.60	5984.25	4231.15	5898.36	2094.65	1727.79	3122.53	3863.59	1840.58	4562.33

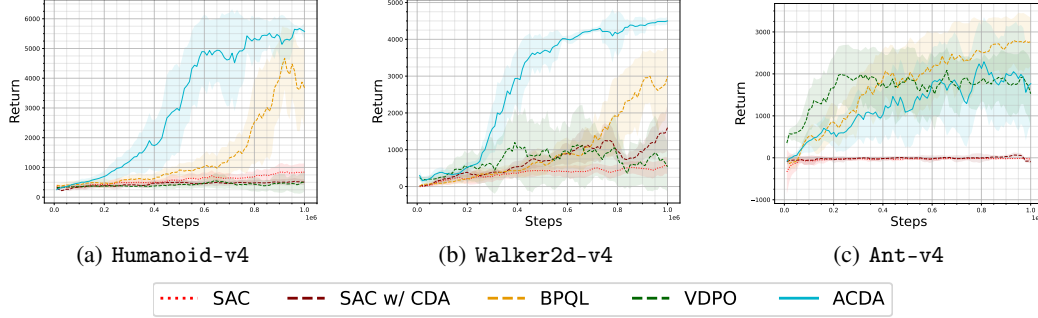


Figure 8: M/M/1 Queue results (all results in Appendix E.1.3). Shaded regions are standard deviation.

As shown in Table 1, ACDA outperforms state-of-the-art in all benchmarks except one, with a significant margin in most cases. The improvement is less substantial in Ant-v4, where performance often overlaps, as indicated by the standard deviation (Figure 8).

6 Conclusion

We introduced the interaction layer, a real-world viable POMDP framework for RL with random unobservable delays. Using the interaction layer, we described and implemented ACDA, a model-based algorithm that significantly outperforms state-of-the-art in delayed RL under random delay processes. Directions of future work include algorithms that can operate on wider areas of delay correlation and on alterations to the interaction layer to handle more complex interaction behavior.

Acknowledgments and Disclosure of Funding

This project was partially supported by the Swedish Research Council (Vetenskapsrådet, grant no. 2024-05043), by Digital Futures (the DLL project and fellowship for Proutiere), by Wallenberg AI, Autonomous Systems and Software Program (WASP) funded by the Knut and Alice Wallenberg Foundation, and by the Vinnova Competence Center for Trustworthy Edge Computing Systems and Applications (TECoSA) at the KTH Royal Institute of Technology. The computations were enabled by resources provided by the National Academic Infrastructure for Supercomputing in Sweden (NAISS), partially funded by the Swedish Research Council through grant agreement no. 2022-06725.

References

- [1] John Schulman et al. “Proximal Policy Optimization Algorithms”. In: *CoRR* abs/1707.06347 (2017). arXiv: 1707.06347. URL: <http://arxiv.org/abs/1707.06347>.
- [2] Tuomas Haarnoja et al. “Soft Actor-Critic: Off-Policy Maximum Entropy Deep Reinforcement Learning with a Stochastic Actor”. In: *Proceedings of the 35th International Conference on Machine Learning*. Ed. by Jennifer Dy and Andreas Krause. Vol. 80. Proceedings of Machine Learning Research. PMLR, Oct. 2018, pp. 1861–1870. URL: <https://proceedings.mlr.press/v80/haarnoja18b.html>.
- [3] D.M. Brooks and C.T. Leondes. “Technical Note - Markov Decision Processes with State-Information Lag”. In: *Operations Research* 20.4 (Aug. 1972), pp. 904–907. DOI: 10.1287/opre.20.4.904.

- [4] Jie Tan et al. *Sim-to-Real: Learning Agile Locomotion For Quadruped Robots*. 2018. arXiv: 1804.10332 [cs.R0].
- [5] Asok Ray. “Distributed data communication networks for real-time process control”. In: *Chemical Engineering Communications* 65.1 (1988), pp. 139–154. DOI: 10.1080/00986448808940249. eprint: <https://doi.org/10.1080/00986448808940249>. URL: <https://doi.org/10.1080/00986448808940249>.
- [6] Rogelio Luck and Asok Ray. “An observer-based compensator for distributed delays”. In: *Automatica* 26.5 (1990), pp. 903–908. ISSN: 0005-1098. DOI: [https://doi.org/10.1016/0005-1098\(90\)90007-5](https://doi.org/10.1016/0005-1098(90)90007-5). URL: <https://www.sciencedirect.com/science/article/pii/0005109890900075>.
- [7] Thomas J. Walsh et al. “Learning and planning in environments with delayed feedback”. In: *Autonomous Agents and Multi-Agent Systems* 18.1 (July 2008), p. 83. ISSN: 1573-7454. DOI: 10.1007/s10458-008-9056-7. URL: <https://doi.org/10.1007/s10458-008-9056-7>.
- [8] Vlad Firoiu, Tina Ju, and Josh Tenenbaum. “At Human Speed: Deep Reinforcement Learning with Action Delay”. In: *CoRR* abs/1810.07286 (2018). arXiv: 1810.07286. URL: <http://arxiv.org/abs/1810.07286>.
- [9] Simon Ramstedt and Chris Pal. “Real-Time Reinforcement Learning”. In: *Advances in Neural Information Processing Systems*. Ed. by H. Wallach et al. Vol. 32. Curran Associates, Inc., 2019. URL: <https://proceedings.neurips.cc/paper/2019/hash/54e36c5ff5f6a1802925ca009f3ebb68-Abstract.html>.
- [10] Baiming Chen et al. “Delay-aware model-based reinforcement learning for continuous control”. In: *Neurocomputing* 450 (Apr. 2021), pp. 119–128. ISSN: 0925-2312. DOI: <https://doi.org/10.1016/j.neucom.2021.04.015>. URL: <https://www.sciencedirect.com/science/article/pii/S0925231221005427>.
- [11] Pierre Liotet et al. “Delayed Reinforcement Learning by Imitation”. In: *Proceedings of the 39th International Conference on Machine Learning*. Ed. by Kamalika Chaudhuri et al. Vol. 162. Proceedings of Machine Learning Research. PMLR, 17–23 Jul 2022, pp. 13528–13556. URL: <https://proceedings.mlr.press/v162/liotet22a.html>.
- [12] Armin Karamzade et al. *Reinforcement Learning from Delayed Observations via World Models*. 2024. arXiv: 2403.12309 [cs.LG]. URL: <https://arxiv.org/abs/2403.12309>.
- [13] Qingyuan Wu et al. “Boosting Reinforcement Learning with Strongly Delayed Feedback Through Auxiliary Short Delays”. In: *Proceedings of the 41st International Conference on Machine Learning*. Ed. by Ruslan Salakhutdinov et al. Vol. 235. Proceedings of Machine Learning Research. PMLR, 21–27 Jul 2024, pp. 53973–53998. URL: <https://proceedings.mlr.press/v235/wu24af.html>.
- [14] Jangwon Kim et al. “Belief Projection-Based Reinforcement Learning for Environments with Delayed Feedback”. In: *Advances in Neural Information Processing Systems*. Ed. by A. Oh et al. Vol. 36. Curran Associates, Inc., 2023, pp. 678–696. URL: https://proceedings.neurips.cc/paper_files/paper/2023/file/0252a434b18962c94910c07cd9a7fecc-Paper-Conference.pdf.
- [15] Qingyuan Wu et al. “Variational Delayed Policy Optimization”. In: *Advances in Neural Information Processing Systems*. Ed. by A. Globerson et al. Vol. 37. Curran Associates, Inc., 2024, pp. 54330–54356. URL: https://proceedings.neurips.cc/paper_files/paper/2024/file/61a18c8a7a1ea7445375dd7255905bc3-Paper-Conference.pdf.
- [16] Yann Bouteiller et al. “Reinforcement Learning with Random Delays”. In: *International Conference on Learning Representations*. 2021. URL: <https://openreview.net/forum?id=QFYnK1BJYR>.
- [17] Mark Towers et al. *Gymnasium: A Standard Interface for Reinforcement Learning Environments*. 2024. arXiv: 2407.17032 [cs.LG]. URL: <https://arxiv.org/abs/2407.17032>.
- [18] K.V. Katsikopoulos and S.E. Engelbrecht. “Markov decision processes with delays and asynchronous cost collection”. In: *IEEE Transactions on Automatic Control* 48.4 (2003), pp. 568–574. DOI: 10.1109/TAC.2003.809799.
- [19] Kurtland Chua et al. “Deep Reinforcement Learning in a Handful of Trials using Probabilistic Dynamics Models”. In: *Advances in Neural Information Processing Systems*. Ed. by S. Bengio et al. Vol. 31. Curran Associates, Inc., 2018. URL: <https://proceedings.neurips.cc/paper/2018/file/3de568f8597b94bda53149c7d7f5958c-Paper.pdf>.

- [20] Wei Wang et al. “Addressing Signal Delay in Deep Reinforcement Learning”. In: *The Twelfth International Conference on Learning Representations*. 2024. URL: <https://openreview.net/forum?id=Z8UfDs4J46>.
- [21] Danijar Hafner et al. “Learning Latent Dynamics for Planning from Pixels”. In: *Proceedings of the 36th International Conference on Machine Learning*. Ed. by Kamalika Chaudhuri and Ruslan Salakhutdinov. Vol. 97. Proceedings of Machine Learning Research. PMLR, Sept. 2019, pp. 2555–2565. URL: <https://proceedings.mlr.press/v97/hafner19a.html>.
- [22] Danijar Hafner et al. “Dream to Control: Learning Behaviors by Latent Imagination”. In: *International Conference on Learning Representations*. 2020. URL: <https://openreview.net/forum?id=S110TC4tDS>.
- [23] Thomas M. Moerland et al. “Model-based Reinforcement Learning: A Survey”. In: *Foundations and Trends® in Machine Learning* 16.1 (2023), pp. 1–118. ISSN: 1935-8237. DOI: 10.1561/22000000086. URL: <http://dx.doi.org/10.1561/22000000086>.
- [24] E. N. Gilbert. “Capacity of a burst-noise channel”. In: *The Bell System Technical Journal* 39.5 (1960), pp. 1253–1265. DOI: 10.1002/j.1538-7305.1960.tb03959.x.
- [25] E. O. Elliott. “Estimates of error rates for codes on burst-noise channels”. In: *The Bell System Technical Journal* 42.5 (1963), pp. 1977–1997. DOI: 10.1002/j.1538-7305.1963.tb00955.x.
- [26] Leonard Kleinrock. *Theory, Volume 1, Queueing Systems*. USA: Wiley-Interscience, 1975. ISBN: 0471491101.
- [27] Dan Hendrycks and Kevin Gimpel. *Gaussian Error Linear Units (GELUs)*. 2023. arXiv: 1606.08415 [cs.LG]. URL: <https://arxiv.org/abs/1606.08415>.

Contents

1	Introduction	1
2	Related Work	3
3	The Interaction Layer	4
3.1	Delayed Markov decision processes	4
3.2	Handling delays via the interaction layer	4
3.3	The POMDP model	6
4	Actor-Critic with Delay Adaptation	6
4.1	Heuristic for Assumed Previous Actions	6
4.2	Model-Based Distribution Agent	7
4.3	Training Algorithm	8
5	Evaluation and Results	9
6	Conclusion	10
A	Constant-Delay Augmentation	16
B	Evaluation Details	17
B.1	Action Noise and Its Effect on Performance	17
B.2	Evaluated Delay Distributions	17
B.3	Hyperparameters and Neural Network Structure	20
B.4	Practical Evaluation Details	21
C	Formal Description of the Interaction Layer POMDP	22
D	Detailed Model Description	24
D.1	Model Components and Objective	24
D.2	Training Algorithm	25
E	Additional Results	26
E.1	Time Series Results	26
E.1.1	Performance Evaluation under the $GE_{1,23}$ Delay Process	27
E.1.2	Performance Evaluation under the $GE_{4,32}$ Delay Process	28
E.1.3	Performance Evaluation under the M/M/1 Queue Delay Process	29
E.2	Model-Based Distribution Agent vs. Adaptiveness	30
E.2.1	Performance of MDA under the $GE_{1,23}$ Delay Process	31
E.2.2	Performance of MDA under the $GE_{4,32}$ Delay Process	32
E.2.3	Performance of MDA under the M/M/1 Queue Delay Process	33
E.3	Results when violating the upper bound assumptions	34

E.3.1	$GE_{1,23}$ Delay Process with Low CDA	35
E.3.2	$GE_{4,32}$ Delay Process with Low CDA	36
E.3.3	M/M/1 Queue Delay Process with Low CDA	37
F	Interaction-Delayed Reinforcement Learning with Real-Valued Delay	38
F.1	Origin and Effect of Delay as Continuous Time	38
F.2	Interaction Layer to Enforce Discrete Delay	39

Outline of the Appendices

Appendix A presents how we implement constant-delay augmentation (CDA) in our framework. This allows agents to act with constant delay using the interaction layer even if the underlying delay process is stochastic. We primarily use this to provide a fair comparison against related work.

Appendix B presents the evaluation details. In Appendix B.1 we demonstrate that stochastic transitions are necessary to see the effects of delay, both theoretically and with an evaluated example. We also show in Appendix B.1 how we use action noise to convert deterministic transitions into stochastic ones. Appendix B.2 describes the delay distributions used in the benchmarks. Lastly, in Appendix B.3 we present the hyperparameters used, and in Appendix B.4 we present the software and hardware used for running the benchmarks.

Appendix C formalizes the interaction layer as a POMDP. This POMDP is used to simulate the interaction layer in the benchmarks.

Appendix D formalizes the model and its objective, as well as providing an expanded version of the algorithm presented in Section 4.3.

Appendix E contains additional results. Appendix E.1 contains all results presented in the conclusion, with time series plots and standard deviation. In Appendix E.2 we evaluate the model-based distribution agent under CDA, showing that it is the adaptiveness that leads to gains in performance rather than the policy itself. In Appendix E.3 we evaluate the effect of using a lower bound for CDA that holds most of the time, but is occasionally violated. The latter two Appendices E.2 and E.3 show that the adaptiveness of the interaction layer offers gains and stability in performance that cannot be obtained by operating in a constant-delay manner.

Appendix F shows an alternative, more realistic definition of delayed MDPs which uses real-valued delays rather than discrete.

A Constant-Delay Augmentation

To be able to evaluate and compare fairly with state-of-the-art algorithms, we make it possible to have constant delay augmentation within our framework. Specifically, to allow algorithms such as BPQL and VDPO that expect a constant delay when the underlying delay process is stochastic, we apply a *constant-delay augmentation* (CDA) on top of the interaction layer. CDA converts the interaction layer POMDP into a constant-delay MDP, under the assumption that the maximum delay does not exceed h steps. This augmentation ensures that we evaluate state-of-the-art as intended when comparing their performance against ACDA.

CDA is implemented on top of the interaction layer by simply arranging the contents of the action packet matrix such that, no matter when action packet \mathbf{a}_t arrives (between $t + 1$ and $t + h$), each action will be executed h steps after it was generated. We illustrate this procedure of constructing the action packet in Algorithm 3.

Algorithm 3 Constant-Delay Augmentation using the Interaction Layer

Input $\mathbf{o}_t = (t, s_t, \mathbf{b}_t, \delta_t, c_t)$ (Observation packet)
 π (Constant-delay policy operating on the horizon h)

1: $a_t, \dots, a_{t+h-1} = \mathbf{b}_t$

2: $a_{t+h} \sim \pi(\cdot | s_t, a_t, \dots, a_{t+h-1})$

3: $\mathbf{a}_t = \left(t, \begin{bmatrix} a_{t+1} & a_{t+2} & a_{t+3} & \cdots & a_{t+h-2} & a_{t+h-1} & a_{t+h} \\ a_{t+2} & a_{t+3} & a_{t+4} & \cdots & a_{t+h-1} & a_{t+h} & a_{t+h} \\ a_{t+3} & a_{t+4} & a_{t+5} & \cdots & a_{t+h} & a_{t+h} & a_{t+h} \\ \vdots & \vdots & \vdots & \ddots & \vdots & \vdots & \vdots \\ a_{t+h-1} & a_{t+h} & a_{t+h} & \cdots & a_{t+h} & a_{t+h} & a_{t+h} \\ a_{t+h} & a_{t+h} & a_{t+h} & \cdots & a_{t+h} & a_{t+h} & a_{t+h} \end{bmatrix} \right)$

4: **return** \mathbf{a}_t

This states that if \mathbf{a}_t arrives at $t + i$, then the actions to be applied are $a_{t+i}, a_{t+\min(h,i+1)}, a_{t+\min(h,i+2)}, \dots, a_{t+\min(h,i+(h-3))}, a_{t+\min(h,i+(h-2))}, a_{t+h}$, which ensures that \mathbf{b}_t always is a correct guess of the actions to be applied next. For $i > 1$, we pad with a_{t+h} to the right on each row to represent the shifting behavior. Forming the action packets in this way ensures that a_{t+h} always gets executed at time $t + h$ given that the delay does not exceed h .

The policy π can be any constant-delay augmented policy. We can also apply the model-based distribution policy from the ACDA algorithm to the CDA setting, by letting $\pi(a_{t+h} | s_t, a_t, \dots, a_{t+h-1}) = \pi_\theta(a_{t+h} | z_h)$, where $z_h = \text{STEP}_\omega^h(\text{EMBED}_\omega(s_t), a_t, \dots, a_{t+h-1})$. We present results of this policy in Appendix E.2.

This assumes the horizon h is a valid upper bound of the delay. We can still perform the augmentation if h is less than the upper bound, but then we are no longer guaranteed the MDP properties of constant delay. We present results of this in Appendix E.3.

B Evaluation Details

This section provides a more complete overview of the evaluation and the results. We provide justification for choosing the 5% noise on environments (Appendix B.1), the delay processes used (Appendix B.2), the hyperparameters used and neural network architectures used (Appendix B.3), as well as the software and hardware used during evaluation (Appendix B.4). The complete results for all benchmarks are presented separately in Appendix E.

B.1 Action Noise and Its Effect on Performance

The benchmark environments used, as defined in Gymnasium, have fully deterministic transitions. As a result, they are theoretically unaffected by delay: the optimal value achievable in the delayed MDP is identical to that of the undelayed MDP. This follows trivially from the fact that, with a perfect deterministic model of the MDP dynamics, the agent can precisely predict the future state in which its action will be applied. Consequently, the agent can plan as if there were no delay at all.

The same is not true for MDPs with stochastic transition dynamics. To show this, consider the MDP with $S = \{H, T\}$, $A = \{H, T\}$, $r(H, H) = 1$, $r(T, T) = 1$, $r(H, T) = 0$, $r(T, H) = 0$, where $\forall s', s, a \quad p(s'|s, a) = 0.5$. This MDP models flipping a fair coin where the agent is given a reward of 1 if it can correctly identify the face of the current coin. Consider this MDP with a constant delay of 1 time step. Now, the agent instead has to guess the face of the next coin, on which it can do no better than a 50/50 guess. Therefore, in this example, the value of an optimal agent in the delayed MDP is half of the value of an optimal agent in the undelayed MDP.

To better highlight the practical issues with delay, we add uncertainty to transitions in the Gymnasium environments by adding noise to the actions prior to being applied to the environment. Let β be the noise factor indicating how much noise we add relative to the span of values that the action can take. Then we add noise to the actions a as follows:

$$\text{Assume } a = [a(1), a(2), \dots, a(n)] \quad (2)$$

$$a(i)_{\max} = \text{maximum value for } a(i) \quad (3)$$

$$a(i)_{\min} = \text{minimum value for } a(i) \quad (4)$$

$$\nu(i) = \beta \cdot (a(i)_{\max} - a(i)_{\min}) \cdot \xi \quad (5)$$

$\xi \sim \mathcal{N}(0,1)$

$$\tilde{a}(i) = \text{clip}(a(i) + \nu(i), a(i)_{\min}, a(i)_{\max}) \quad (6)$$

$$\tilde{a} = [\tilde{a}(1), \tilde{a}(2), \dots, \tilde{a}(n)] \quad (7)$$

Here we assume that the actions are continuous, which works since all environments in our evaluation are of this nature. Then the transitions become $p(s'|s, \tilde{a})$, with the noisy action applied instead of the original one. We use the noise factor $\beta = 0.05$ in all our noisy environments evaluated here.

To see the effect that this noise has on delayed RL in practice, we evaluate the performance of BPQL over different delays, with and without noise, and compare the results in Figure 9. As is explained later in Appendix B.4, we reimplement the BPQL training algorithm in our training framework.

The results without noise for delays 3, 6, and 9, shown in Figure 9, closely match those reported by Kim et al. [14] (8100 ± 543.4 , 6334.6 ± 245.3 , and 5887.5 ± 270.5 for delays 3, 6, and 9 respectively). This suggests that our implementation is faithful to their approach. Notably, we observe that in the deterministic setting, the impact of delay, while causing a significant initial drop in performance, does not lead to further degradation over longer time horizons. This behavior contrasts with the noisy environment, where performance continues to decline more noticeably over time.

We therefore conclude that a fair evaluation of delayed RL should be done in environments with stochastic dynamics.

B.2 Evaluated Delay Distributions

As mentioned in Section 5, we evaluate on delay processes following the Gilbert-Elliot and M/M/1 models. We formally define these processes in this section as well as the conservative and optimistic

Delay	Without Noise	Noisy
3	7839.43 \pm 137.78	7338.29 \pm 122.52
6	6316.15 \pm 61.05	5405.36 \pm 224.25
9	5948.43 \pm 60.29	5024.68 \pm 236.23
12	6010.61 \pm 63.67	4549.05 \pm 273.90
15	5692.23 \pm 39.43	4904.58 \pm 106.58
18	5760.71 \pm 46.72	4260.58 \pm 126.20
21	5763.55 \pm 44.03	4772.30 \pm 664.66
24	5579.54 \pm 58.32	4018.73 \pm 525.76

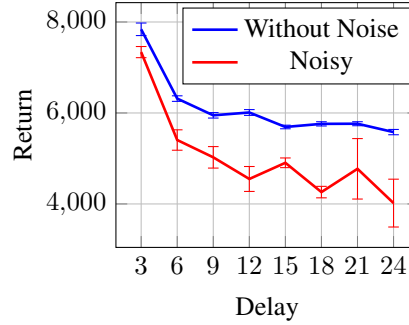


Figure 9: HalfCheetah-v4 performance on BPQL with delay and noise. Showing the best evaluated average return over a training period of 1 million time-steps for each value of delay, with and without noise.

worst-case delay assumptions (high and low CDA). Appendix E.2 and E.3 evaluate the performance under high and low CDA, respectively.

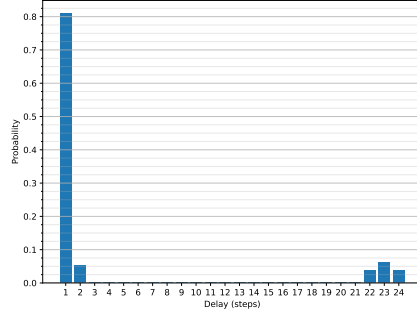
We consider $GE_{1,23}$ and $GE_{4,32}$, two Gilbert-Elliot models. These are Markovian processes alternating between two states, a good state s_{good} and a bad state s_{bad} . We describe the models in Table 2 as a two-state Markov process, where they initially start in the good state. The notation $D(d|s)$ is used to describe the probability of sampling the delay d in the Gilbert-Elliot state s . We set the opportunistic low CDA to be the maximum delay that can be sampled in the s_{good} state.

Table 2: Description of the Gilbert-Elliot delay processes used during evaluation.

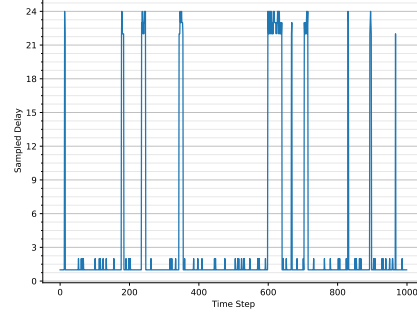
Property	$GE_{1,23}$	$GE_{4,32}$
$p(s_{\text{bad}} s_{\text{good}})$	$\frac{1}{125}$	$\frac{1}{250}$
$p(s_{\text{good}} s_{\text{bad}})$	$\frac{1}{20}$	$\frac{1}{32}$
$D(d s_{\text{good}})$	$\Pr[d = 1] = \frac{15}{16}$ $\Pr[d = 2] = \frac{1}{16}$	$\Pr[d = 4] = 1$
$D(d s_{\text{bad}})$	$\Pr[d = 22] = \frac{3}{11}$ $\Pr[d = 23] = \frac{5}{11}$ $\Pr[d = 24] = \frac{3}{11}$	$\Pr[d = 32] = 1$
Low CDA	2	4
High CDA	24	32

We plot the distribution histogram and time series over 1000 samples of the Gilbert-Elliot processes in Figure 10.

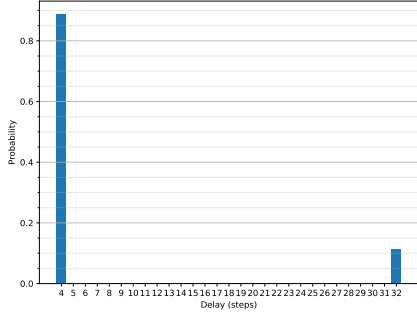
The M/M/1 queue process is described by simulating an M/M/1 queue according to the pseudocode in Algorithm 4. We set the arrival rate $\lambda_{\text{arrive}} = 0.33$ and the service rate $\lambda_{\text{service}} = 0.75$. The arrivals and departures are dictated by independent Poisson processes parametrized by these values (e.g., the time between two arrivals is a r.v. with exponential distribution of mean λ_{arrive}). Note that there is no upper bound on this delay process, and it is therefore impossible to convert this to a constant-delay MDP through Constant Delay Augmentation (CDA). We can still apply the CDA conversion from Appendix A to apply constant-delay methodologies on this delay process, though they are no longer operating on an MDP.



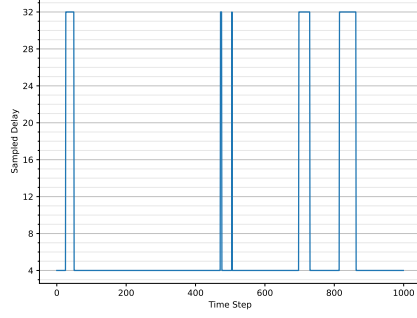
(a) $GE_{1,23}$ distribution histogram



(b) $GE_{1,23}$ distribution time series



(c) $GE_{4,32}$ distribution histogram



(d) $GE_{4,32}$ distribution time series

Figure 10: The Gilbert-Elliot delay processes.

Algorithm 4 M/M/1 Queue Delay Generator

Initial State: $t_{\text{arrival}} \sim \text{Exp}(\cdot | \lambda_{\text{arrive}})$ (Time of arrival of the first packet)
 $t_{\text{service}} \leftarrow \emptyset$ (Cannot serve anything yet)
 $Q \leftarrow \text{FIFOqueue}()$ (Empty queue initially)

```

1: procedure SAMPLEDELAY
2:   if  $t_{\text{service}} = \emptyset$  then
3:      $t \leftarrow t_{\text{arrival}}$ 
4:      $Q.\text{insert}(t)$ 
5:      $t_{\text{arrival}} \sim \text{Exp}(\cdot | \lambda_{\text{arrive}}) + t$ 
6:      $t_{\text{service}} \sim \text{Exp}(\cdot | \lambda_{\text{service}}) + t$ 
7:   while  $t_{\text{arrival}} < t_{\text{service}}$  do
8:      $t \leftarrow t_{\text{arrival}}$ 
9:      $Q.\text{insert}(t)$ 
10:     $t_{\text{arrival}} \sim \text{Exp}(\cdot | \lambda_{\text{arrive}}) + t$ 
11:   $t \leftarrow t_{\text{service}}$ 
12:   $t_{\text{inserted}} \leftarrow Q.\text{pop}()$ 
13:   $d \leftarrow \lceil t - t_{\text{inserted}} \rceil$ 
14:  if  $Q.\text{isempty}()$  then
15:     $t_{\text{service}} \leftarrow \emptyset$ 
16:  else
17:     $t_{\text{service}} \sim \text{Exp}(\cdot | \lambda_{\text{service}}) + t$ 
18:  return  $d$ 

```

We plot delays of the M/M/1 queue in Figure 11. We set the conservative delay (high CDA) to be 16, and the opportunistic delay (low CDA) to be 4 for the M/M/1 queue.

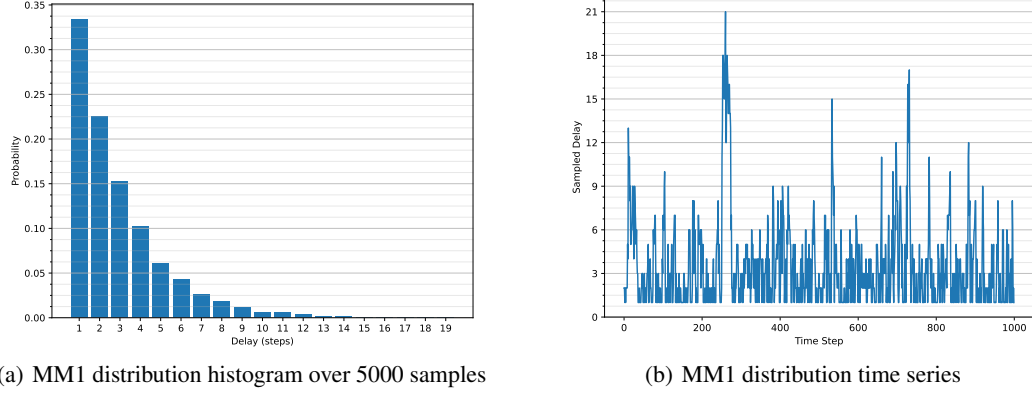


Figure 11: Delays from an M/M/1 queue when $\lambda_{\text{arrive}} = 0.33$ and $\lambda_{\text{service}} = 0.75$.

B.3 Hyperparameters and Neural Network Structure

Hyperparameters used for training the policy π_θ and the critic Q_ϕ in ACDA follow the common learning rates used for SAC, and is therefore shared between SAC, BPQL, and ACDA. We show these together with the model hyperparameters used for ACDA in Tables 3(a) and 3(b). The hyperparameters for the model share the same replay size and batch size. We use slightly different parameters for the model when learning the dynamics on the 2D environments (HalfCheetah-v4, Hopper-v4, and Walker2d-v4) and the 3D environments (Ant-v4 and Humanoid-v4).

Table 3(a): SAC Hyperparameters

Parameter	Value
Policy (θ) learning rate	$3 \cdot 10^{-4}$
Critic (ϕ) Learning rate	$3 \cdot 10^{-4}$
Temperature (α) learning rate	$3 \cdot 10^{-4}$
Starting temperature (α)	0.2
Temperature threshold \mathcal{H}	$-\dim(A)$
Target smoothing coefficient	0.005
Replay buffer size	10^6
Discount γ	0.99
Minibatch size	256
Optimizer (policy, critic, temp.)	Adam
Activation (policy, critic)	ReLU

Table 3(b): Model Hyperparameters

Parameter	Value (2D)	Value (3D)
Model (ω) learning rate	10^{-4}	$5 \cdot 10^{-5}$
Model training window n	16	16
Latent GRU dimensionality	384	512
Angle clamping	Yes	No
Optimizer	Adam	Adam
Activation	ClipSiLU	ClipSiLU

The π_θ , Q_ϕ , and EMBED_ω networks are all implemented as MLPs with 2 hidden layers of dimension 256 each. The policy output the mean and standard deviation of a gaussian distribution, which is put through tanh and scaled to exactly cover the action space. The EMIT_ω network consists of 2 common layers of dimension 256 each, with additional "head" layers of dimension 256 each for outputting the mean and standard deviation of a gaussian distribution.

Both MLPs in the model make use of a clipped version of SiLU [27] as its activation function, where $\text{ClipSiLU}(x) = \text{SiLU}(\max(-20, x))$. We found that the use of ClipSiLU significantly improved the model performance. Earlier experiments with models using ReLU activation did not manage to achieve good performance when used with ACDA.

The angle clamping mentioned in Table 3(b) constrains all components of the state space that represent an angle to reside in the range $[-\pi, \pi)$. We only apply this to 2D environments.

The model is trained using sub-trajectories $T_n = (s_t, a_t, s_{t+1}, a_{t+1}, \dots, s_{t+n-1}, a_{t+n-1}, s_{t+n})$, where n is the model training window in Table 3(b). We optimize the model parameters ω with with sub-trajectories using the following equation

$$\nabla_{\omega} \mathbb{E}_{T_n \sim \mathcal{R}} \left[\frac{1}{n+1} \sum_{k=0}^n -\log \text{EMIT}_{\omega}(s_{t+k} | \text{STEP}_{\omega}^k(\text{EMBED}_{\omega}(s_t), a_t, \dots, a_{t+k-1})) \right] \quad (8)$$

where for $k = 0$, we just evaluate the embedder as $\text{EMIT}_{\omega}(s_t | \text{EMBED}_{\omega}(s_t))$.

B.4 Practical Evaluation Details

We use PyTorch for deep RL functionality and Gymnasium for RL functionality. The interaction layer is implemented as a Gymnasium environment wrapper, based on the formalism described in Appendix C, that extends the Gymnasium API to support action and observation packets. The constant-delay augmentation (CDA) in Appendix A is implemented as a wrapper on top of the interaction layer wrapper, reducing the API back to the original Gymnasium API. We implement ACDA to explicitly make use of the extended interaction layer definitions, whereas we implement BPQL and SAC w/ CDA to operate directly on the regular Gymnasium API using the CDA wrapper. A pass-through wrapper for the interaction layer is used for evaluating SAC without CDA, where the action packet is filled up with the provided action.

For VDPO we reuse the code artifact from their original article. Modifications to their implementation include the addition of action noise, our interaction layer wrappers, and additional statistical reporting. These modifications are documented in the artifact.

All necessary dependencies are provided as conda YAML files.

Each benchmark, meaning a single algorithm training on a single environment with a single delay process, is run using a single Nvidia A40 GPU and 16 CPU cores. ACDA and VDPO benchmarks take around 18-24 hours each to complete. BPQL and SAC benchmarks take around 6 hours each to complete.

C Formal Description of the Interaction Layer POMDP

This section describes the POMDP of the interaction layer introduced in Section 3.3. The POMDP formalizes the interaction between the agent and the interaction layer that is wrapping the underlying system. We assume that the underlying system can be described by an MDP $\mathcal{M} = (S, A, r, p, \mu)$ where S is the state space, A the action space, $r(s, a)$ the reward function, $p(s'|s, a)$ the transition distribution, and $\mu(s)$ the initial state distribution.

The interaction layer wraps the MDP \mathcal{M} , where the interaction delay is described by the delay process D . To fully define the POMDP of the interaction layer, we also need the action buffer horizon h as well as the default action a_{init} . Given this information, the POMDP is described as the tuple $\mathcal{P} = (\mathcal{S}, \mathcal{A}, \mathcal{p}, \mathcal{r}, \mathcal{\mu}, \Omega, O)$. We use the notation $s \in \mathcal{S}$, $\mathbf{a} \in \mathcal{A}$, and $\mathbf{o} \in \Omega$ to denote members of these sets. We also refer to items $\mathbf{a} \in \mathcal{A}$ as *action packets* and items $\mathbf{o} \in \Omega$ as *observation packets*.

An observation is described as the tuple $\mathbf{o} = (t, s, \mathbf{b}, \delta, c)$. This describes the state at the interaction layer at time t , where

- t is the time at the interaction layer when the observation was generated,
- s the underlying system state observed at the same time step,
- $\mathbf{b} = (b_1, b_2, \dots, b_h)$ are the contents of the action buffer at time t (b_1 will immediately be applied to s),
- δ is the delay of the action packet used to update the action buffer \mathbf{b} , and
- c is number of time steps without a new action packet replacing the action buffer contents.

When referring to the state of the action buffer at different time steps, e.g. \mathbf{b}_t and \mathbf{b}_{t+1} , we use the notation $b_{t,i}$ and $b_{t+1,i}$ to refer to the i -th action in \mathbf{b}_t and \mathbf{b}_{t+1} respectively.

The individual components of \mathcal{P} are defined in Equations 9-18:

$$\text{Action space } \mathcal{A} = \mathbb{N} \times \bigcup_{k=1}^{\infty} A^{k \times h} \quad (9)$$

$$\text{Observation space } \Omega = \mathbb{N} \times S \times A^h \times \mathbb{Z}^+ \times \mathbb{N} \quad (10)$$

$$\text{State space } \mathcal{S} = \Omega \times 2^{(\mathbb{Z}^+ \times \mathcal{A})} \quad (11)$$

$$\text{Initial state distribution } \mathcal{\mu}(s) = \begin{cases} \mu(s) & \text{if } s = ((0, s, (a_{\text{init}}, \dots), 1, 0), \emptyset) \\ 0 & \text{otherwise} \end{cases} \quad (12)$$

$$\text{Observation distribution } O(\mathbf{o}|s) = \begin{cases} 1 & \text{if } s = (\mathbf{o}, \mathcal{I}) \\ 0 & \text{otherwise} \end{cases} \quad (13)$$

$$\begin{aligned} \text{Reward function } \mathcal{r}(s_t, \mathbf{a}_t) &= r(s_t, b_1) \\ \text{where } s_t &= ((t, s_t, (b_1, b_2, \dots, b_h), d_t, \delta_t), \mathcal{I}_t) \end{aligned} \quad (14)$$

Equation 11 defines states as tuples $s_t = (\mathbf{o}_t, \mathcal{I}_t)$, where \mathbf{o}_t is the state of the interaction layer (observable) and \mathcal{I}_t is the set of action packets in transit (not observable). The transit set $\mathcal{I}_t \in 2^{(\mathbb{Z}^+ \times \mathcal{A})}$ contains tuples of action packets and their arrival time.

Note that, by the definition of $\mathcal{\mu}$ in Equation 12, we can always check if the action buffer contains the initial actions by $t - (\delta_t + c_t) < 0$. This holds true until the first action packet is received.

The transition dynamics $\mathcal{p}(s_{t+1}|s_t, \mathbf{a}_t)$ are described in Equation 18 below. While this is simple to describe in text and with examples, it becomes complicated to define formally. We first define the a couple of auxiliary functions below to help defining the transition dynamics. We define the function $\text{TRANSMIT}(\mathcal{I}_t, \mathbf{a}_t, d)$ that adds the action \mathbf{a}_t with delay d the transit set, together with the $\min \mathcal{I}$ and $\min_t \mathcal{I}$ operations to get the action packet with nearest arrival:

$$\text{TRANSMIT}(\mathcal{I}_t, \mathbf{a}_t, d) = \{(t + d, \mathbf{a}_t)\} \cup \{(t', \mathbf{a}') \in \mathcal{I}_t : t' < t + d\} \quad (15)$$

$$\min_t \mathcal{I} = \min\{t' : (t', \mathbf{a}') \in \mathcal{I}\} \quad (16)$$

$$\min \mathcal{I} = \begin{cases} \emptyset & \text{if } \mathcal{I} = \emptyset \\ (t', \mathbf{a}') \in \mathcal{I} & \text{if } t' = \min_t \mathcal{I} \end{cases} \quad (17)$$

One aspect of the behavior of the interaction layer, modeled by the $\text{TRANSMIT}(\mathcal{I}_t, \mathbf{a}_t, d)$ function in Equation 15, is that outdated action packets arriving at the interaction layer will be discarded. For example, if \mathbf{a}_t has delay $d_t = 4$, and \mathbf{a}_{t+1} has delay $d_{t+1} = 2$, then \mathbf{a}_{t+1} will arrive at time $t + 3$, whereas \mathbf{a}_t will arrive after at time $t + 4$. When \mathbf{a}_t arrives, the interaction layer will see that the contents of the action buffer is based on information from \mathbf{o}_{t+1} , whereas the action packet \mathbf{a}_t is based on information from \mathbf{o}_t . Therefore, \mathbf{a}_t is considered outdated and will be discarded. Also note that a consequence of this is that d_t will never be observed, not even in hindsight.

Using these functions, we define the transition probabilities below in Equation 18. The probabilities themselves are simple to describe as $p(s_{t+1}|s_t, b_1) \times D(d)$, the complexity arises from checking that the new POMDP state is compatible with the possible sampled delays. The first case covers when no new action packet arrives at the interaction layer at time $t + 1$, the second case when the received action packet \mathbf{a}_t has too few rows in the matrix to update the action buffer for the sampled delay d , and the third case is when a received action packet is used to update the action buffer.

$$p(s_{t+1}|s_t, \mathbf{a}_t) = \begin{cases} p(s_{t+1}|s_t, b_1) \cdot D(d) & \text{if } \mathcal{I}_{t+1} = \text{TRANSMIT}(\mathcal{I}_t, \mathbf{a}_t, d) \wedge \min_t \mathcal{I}_{t+1} > t + 1 \wedge \\ & c_{t+1} = c_t + 1 \wedge \delta_{t+1} = \delta_t \wedge \\ & \mathbf{b}_{t+1} = (b_2, b_3, \dots, b_{h-1}, b_h, b_h) \\ p(s_{t+1}|s_t, b_1) \cdot D(d) & \text{if } \mathcal{I}_{t+1} = \mathcal{I}_{\text{cand}} \setminus \{\min \mathcal{I}_{\text{cand}}\} \wedge \min_t \mathcal{I}_{\text{cand}} = t + 1 \wedge \\ & (t + 1 - u) > L \wedge c_{t+1} = c_t + 1 \wedge \delta_{t+1} = \delta_t \wedge \\ & \mathbf{b}_{t+1} = (b_2, b_3, \dots, b_{h-1}, b_h, b_h) \\ & \text{where } \mathcal{I}_{\text{cand}} = \text{TRANSMIT}(\mathcal{I}_t, \mathbf{a}_t, d) \\ & (t + 1, \mathbf{a}_u) = \min \mathcal{I}_{\text{cand}} \\ & (u, M^u) = \mathbf{a}_u \\ & M^u \in A^{L \times h} \\ p(s_{t+1}|s_t, b_1) \cdot D(d) & \text{if } \mathcal{I}_{t+1} = \mathcal{I}_{\text{cand}} \setminus \{\min \mathcal{I}_{\text{cand}}\} \wedge \min_t \mathcal{I}_{\text{cand}} = t + 1 \wedge \\ & (t + 1 - u) \leq L \wedge c_{t+1} = 0 \wedge \delta_{t+1} = (t + 1 - u) \wedge \\ & \mathbf{b}_{t+1} = M_{(t+1-u)}^u \\ & \text{where } \mathcal{I}_{\text{cand}} = \text{TRANSMIT}(\mathcal{I}_t, \mathbf{a}_t, d) \\ & (t + 1, \mathbf{a}_u) = \min \mathcal{I}_{\text{cand}} \\ & (u, M^u) = \mathbf{a}_u \\ & M^u \in A^{L \times h} \\ 0 & \text{otherwise} \end{cases} \quad (18)$$

where $s_t = (\mathbf{o}_t, \mathcal{I}_t)$

$$s_{t+1} = (\mathbf{o}_{t+1}, \mathcal{I}_{t+1})$$

$$\mathbf{o}_t = (t, s_t, \mathbf{b}_t, \delta_t, c_t)$$

$$\mathbf{o}_{t+1} = (t + 1, s_{t+1}, \mathbf{b}_{t+1}, \delta_{t+1}, c_{t+1})$$

$$\mathbf{b}_t = (b_1, b_2, \dots, b_{h-2}, b_{h-1}, b_h)$$

D Detailed Model Description

This section provides formal definitions of the model introduced in Section 4.2, as well as a detailed definition of the training algorithm presented in Section 4.3. Appendix D.1 presents the formal model definition. Appendix D.2 presents the full training algorithm.

We use the variables θ , ϕ , and ω to denote the parameters of the policy, critic, and model respectively. In practice, these are large vectors of real numbers where different parts of the vector contains the parameters for components in a deep neural network.

D.1 Model Components and Objective

The primary purpose of the model is used to get around the limitation on fixed-size inputs of MLPs. The idea is that, instead of generating actions directly with the augmented state input:

$$a_{t+k} \sim \pi_\theta(\cdot | s_t, a_t, a_{t+1}, \dots, a_{t+k-1}), \quad (19)$$

we generate actions using the distribution over the state that the action will be applied to as policy input:

$$a_{t+k} \sim \pi_\theta(\cdot | p(\cdot | s_t, a_t, a_{t+1}, \dots, a_{t+k-1})), \quad (20)$$

where $p(\cdot | s_t, a_t, a_{t+1}, \dots, a_{t+k-1})$ represents the distribution over states after applying the action sequence $a_t, a_{t+1}, \dots, a_{t+k-1}$ in order to the state s_t . We represent $p(\cdot | s_t, a_t, a_{t+1}, \dots, a_{t+k-1})$ as a fixed-size latent representation, and thanks to this representation, we can generate actions with MLPs for variable size inputs. The purpose of the model is to create these embeddings (defining the mapping between $p(\cdot | s_t, a_t, a_{t+1}, \dots, a_{t+k-1})$ and the corresponding latent representation). Since this kind of policy makes decisions using a distribution over the state, and that the distribution is embedded as a latent representation using a model, we refer to agents using this kind of policy as *model-based distribution agents* (MDA).

The model consists of three components: $\text{EMBED}_\omega(s_t)$, $\text{STEP}_\omega(z_i, a_{t+i})$, and $\text{EMIT}_\omega(\hat{s}_{t+i} | z_{t+i})$.

$\text{EMBED}_\omega(s_t)$ embeds the state s_t into a latent representation z_0 . In a perfect model, z_0 would be an embedding of the Dirac delta distribution $\delta(x - s_t)$.

$\text{STEP}_\omega(z_i, a_{t+i})$ updates the latent representation z_i to include information about what happens if the action a_{t+i} also is applied. Such that, if z_i is a latent representation of $p(\cdot | s_t, a_t, \dots, a_{t+i-1})$, then $z_{i+1} = \text{STEP}_\omega(z_i, a_{t+i})$ is a latent representation of $p(\cdot | s_t, a_t, \dots, a_{t+i-1}, a_{t+i})$.

$\text{EMIT}_\omega(\hat{s}_{t+i} | z_{t+i})$ converts the latent representation z_{t+i} back to a regular parameterized distribution. We use a normal distribution in our model, where EMIT_ω outputs the mean and standard deviation for each component of the MDP state. We never sample from this distribution. This component is only used to ensure that we have a good latent representation.

To make the notation more compact, we use the multi-step notation STEP_ω^k where

$$\text{STEP}_\omega^0(z) = z \quad (21)$$

$$\text{STEP}_\omega^k(z, a_0, a_1, \dots, a_{k-1}) = \text{STEP}_\omega^{k-1}(\text{STEP}_\omega(z, a_0), a_1, \dots, a_{k-1}) \quad (22)$$

With this notation, we say that $\text{STEP}_\omega^k(\text{EMBED}_\omega(s_t), a_t, a_{t+1}, \dots, a_{t+k-1})$ embeds the distribution $p(\cdot | s_t, a_t, a_{t+1}, \dots, a_{t+k-1})$. We optimize the model to minimize the KL-divergence between the embedded distribution and the true distribution. That is

$$\min_{\omega} D_{\text{KL}}(p(\cdot | s_t, a_t, \dots, a_{t+n-1}) \| \text{EMIT}_\omega(\cdot | \text{STEP}_\omega^n(\text{EMBED}_\omega(s_t), a_t, \dots, a_{t+n-1}))) \quad (23)$$

for all possible states s_t and sequences of actions a_t, \dots, a_{t+n-1} . The loss function $\mathcal{L}(\omega)$ from Section 4.2 is a Monte Carlo estimate of this objective:

$$\begin{aligned} \mathcal{L}(\omega) &= \mathbb{E}_{(s_t, a_t, a_{t+1}, \dots, a_{t+n-1}, s_{t+n}) \sim \mathcal{R}} [-\log \text{EMIT}_\omega(s_{t+n} | z_n)] \\ \text{where } z_n &= \text{STEP}_\omega^n(\text{EMBED}_\omega(s_t), a_t, a_{t+1}, \dots, a_{t+n-1}) \\ &\text{and } \mathcal{R} \text{ is a replay buffer with experiences collected online.} \end{aligned} \quad (24)$$

D.2 Training Algorithm

This section presents the full version of the training algorithm from Section 4.3. As with SAC, we assume that π_θ is represented as a reparameterizable policy that is a deterministic function with independent noise input.

Algorithm 5 Actor-Critic with Delay Adaptation

```

1: Initialize policy  $\pi_\theta$ , critics  $Q_{\phi_1}, Q_{\phi_2}$ , model  $\omega$ , temperature  $\alpha$ , target networks  $\phi'_1, \phi'_2$ , and replay
    $\mathcal{R}$ 
2: for each epoch do
3:   // Stage 1: Sample trajectory
4:   Collected trajectory:  $\mathcal{T} = \emptyset$ 
5:    $t \leftarrow 0$ 
6:   Reset interaction layer state:  $s_0 \sim \mu$ , Observe  $\mathbf{o}_0$ 
7:   while terminal state not reached do
8:      $(t, s_t, \mathbf{b}_t, \delta_t, c_t) = \mathbf{o}_t$ 
9:     for  $k \leftarrow 1$  to  $L$  do
10:      Select  $\hat{a}_1^{t+k}, \dots, \hat{a}_h^{t+k}$  by Algorithm 1
11:       $y_0 \leftarrow (\hat{a}_1^{t+k}, \dots, \hat{a}_h^{t+k})$ 
12:      for  $i \leftarrow 1$  to  $h$  do
13:         $a_i^{t+k} \sim \pi_\theta(\cdot | \text{STEP}_\omega^{k+i-1}(\text{EMBED}_\omega(s_t), y_{i-1}))$ 
14:         $y_i \leftarrow (y_{i-1}, a_i^{t+k})$ 
15:       $\mathbf{a}_t \leftarrow \left( t, \begin{bmatrix} a_1^{t+1} & a_2^{t+1} & a_3^{t+1} & \dots & a_h^{t+1} \\ a_1^{t+2} & a_2^{t+2} & a_3^{t+2} & \dots & a_h^{t+2} \\ \vdots & \vdots & \vdots & \ddots & \vdots \\ a_1^{t+L} & a_2^{t+L} & a_3^{t+L} & \dots & a_h^{t+L} \end{bmatrix} \right)$ 
16:      Send  $\mathbf{a}_t$  to interaction layer, observe  $r_t, \mathbf{o}_{t+1}, \Gamma_{t+1}$ 
17:      Add  $(\mathbf{o}_t, \mathbf{a}_t, r_t, \mathbf{o}_{t+1}, \Gamma_{t+1})$  to  $\mathcal{T}$ 
18:       $t \leftarrow t + 1$ 
19:   // Stage 2: Reconstruct transition info
20:   for  $(\mathbf{o}_i, \mathbf{a}_i, r_i, \mathbf{o}_{i+1}, \Gamma_{i+1}) \in \mathcal{T}$  do
21:      $(i, s_i, \mathbf{b}_i, \delta_i, c_i) = \mathbf{o}_i, \quad (i+1, s_{i+1}, \mathbf{b}_{i+1}, \delta_{i+1}, c_{i+1}) = \mathbf{o}_{i+1}$ 
22:      $a_i = b_{i,1}$ 
23:     if  $i - (\delta_i + c_i) \geq 0$  then
24:       // (Recover the input used by  $\pi_\theta$  and  $\text{STEP}_\omega^k$  to generate  $b_{i,1}$  and  $b_{i+1,1}$ )
25:        $j \leftarrow i - (\delta_i + c_i), \quad j' \leftarrow (i+1) - (\delta_{i+1} + c_{i+1})$ 
26:       Reconstruct  $\hat{a}_1^{j+\delta_i}, \dots, \hat{a}_{\delta_i}^{j+\delta_i}$ , choose  $a_1^{j+\delta_i}, \dots, a_{c_i}^{j+\delta_i}$  from  $\mathbf{a}_j$ 
27:       Reconstruct  $\hat{a}_1^{j'+\delta_{i+1}}, \dots, \hat{a}_{\delta_{i+1}}^{j'+\delta_{i+1}}$ , choose  $a_1^{j'+\delta_{i+1}}, \dots, a_{c_{i+1}}^{j'+\delta_{i+1}}$  from  $\mathbf{a}_{j'}$ 
28:        $y_i \leftarrow (\hat{a}_1^{j+\delta_i}, \dots, \hat{a}_{\delta_i}^{j+\delta_i}, a_1^{j+\delta_i}, \dots, a_{c_i}^{j+\delta_i})$ 
29:        $y_{i+1} \leftarrow (\hat{a}_1^{j'+\delta_{i+1}}, \dots, \hat{a}_{\delta_{i+1}}^{j'+\delta_{i+1}}, a_1^{j'+\delta_{i+1}}, \dots, a_{c_{i+1}}^{j'+\delta_{i+1}})$ 
30:       // We denote their lengths as  $|y_i| = \delta_i + c_i$ 
31:       Add  $(s_i, \mathbf{a}_i, r_i, s_{i+1}, \Gamma_{i+1}, y_i, y_{i+1})$  to  $\mathcal{R}$ 
32:   // Stage 3: Update network weights
33:   for  $|\mathcal{T}|$  sampled batches of  $(s, a, r, s', \Gamma, y, y')$  from  $\mathcal{R}$  do
34:     // These are computed in expectation of samples from  $\mathcal{R}$ 
35:      $\hat{a}' \sim \pi_\theta(\cdot | \text{STEP}_\omega^{|y'|}(\text{EMBED}_\omega(s'), y'))$ 
36:      $x = r + \gamma(1 - \Gamma)(\min(Q_{\phi'_1}(s', \hat{a}'), Q_{\phi'_2}(s', \hat{a}') - \alpha \log \pi_\theta(\hat{a}' | \dots)))$ 
37:     Do gradient descent step on  $\nabla_{\phi_1}(Q_{\phi_1}(s, a) - x)^2$  and  $\nabla_{\phi_2}(Q_{\phi_2}(s, a) - x)^2$ 
38:      $\hat{a} \sim \pi_\theta(\cdot | \text{STEP}_\omega^{|y|}(\text{EMBED}_\omega(s), y))$ 
39:     Do gradient ascent step on  $\nabla_\theta(\min(Q_{\phi_1}(s, \hat{a}), Q_{\phi_2}(s, \hat{a})) - \alpha \log \pi_\theta(\hat{a} | \dots))$ 
40:     Update  $\alpha$  according to SAC
41:     Compute  $\nabla_\omega$  by Equation 8 and do gradient descent step
42:     Update target networks  $\phi'_1, \phi'_2$ 

```

E Additional Results

This section presents additional results to complement those presented in Section 5. Appendix E.1 presents the results from Table 1 as time series plots, showing how the mean and standard deviation of the evaluated return changes over the training process.

Appendix E.2 and E.3 answers two questions that is not part of the evaluation in Section 5. The questions that these appendices answer are:

- Appendix E.2 answers the question whether the gain in performance is due to the model-based policy introduced in Section 4.2 or due to the adaptiveness of ACDA. We evaluate this by modifying the BPQL algorithm such that it uses the MDA policy instead of a direct MLP policy, and compare how that performs against ACDA. The results clearly shows that it is the adaptiveness of the interaction layer that is the reason for the strong performance of ACDA.
- Appendix E.3 answers the question whether acting with CDA under a different horizon h than the worst-case delay is better than trying to adapt to varying delays. We set up this demonstration by applying CDA with a horizon h that is greater than or equal to sampled delay most of the time, but occasionally a sampled delay exceeds this horizon. This kind of CDA does not result in a constant-delay MDP that BPQL and VDPO expects, hence we did not include this in the main evaluation. The results in Appendix E.3 shows that while VDPO and BPQL occasionally gains performance in this setting, ACDA is still the best performing algorithm in most cases. ACDA is always close to the highest performing algorithm in the few cases where ACDA does not achieve the best mean return. These results shows that the adaptiveness of the interaction layer provides an increase in performance that cannot be achieved through constant-delay approaches.

E.1 Time Series Results

This section presents the results from the evaluation in Section 5 as time series plots, including standard deviation bands. Unless otherwise specified, the evaluation methodology follows that described in Section 5. To reduce noise and highlight trends, each time series is smoothed using a running average over five evaluation points.

The results in this appendix is split into the delay processes used. Appendix E.1.1 presents results for the $GE_{1,23}$ delay process, Appendix E.1.2 for the $GE_{4,32}$ delay process, and Appendix E.1.3 for the M/M/1 queue delay process.

E.1.1 Performance Evaluation under the $GE_{1,23}$ Delay Process

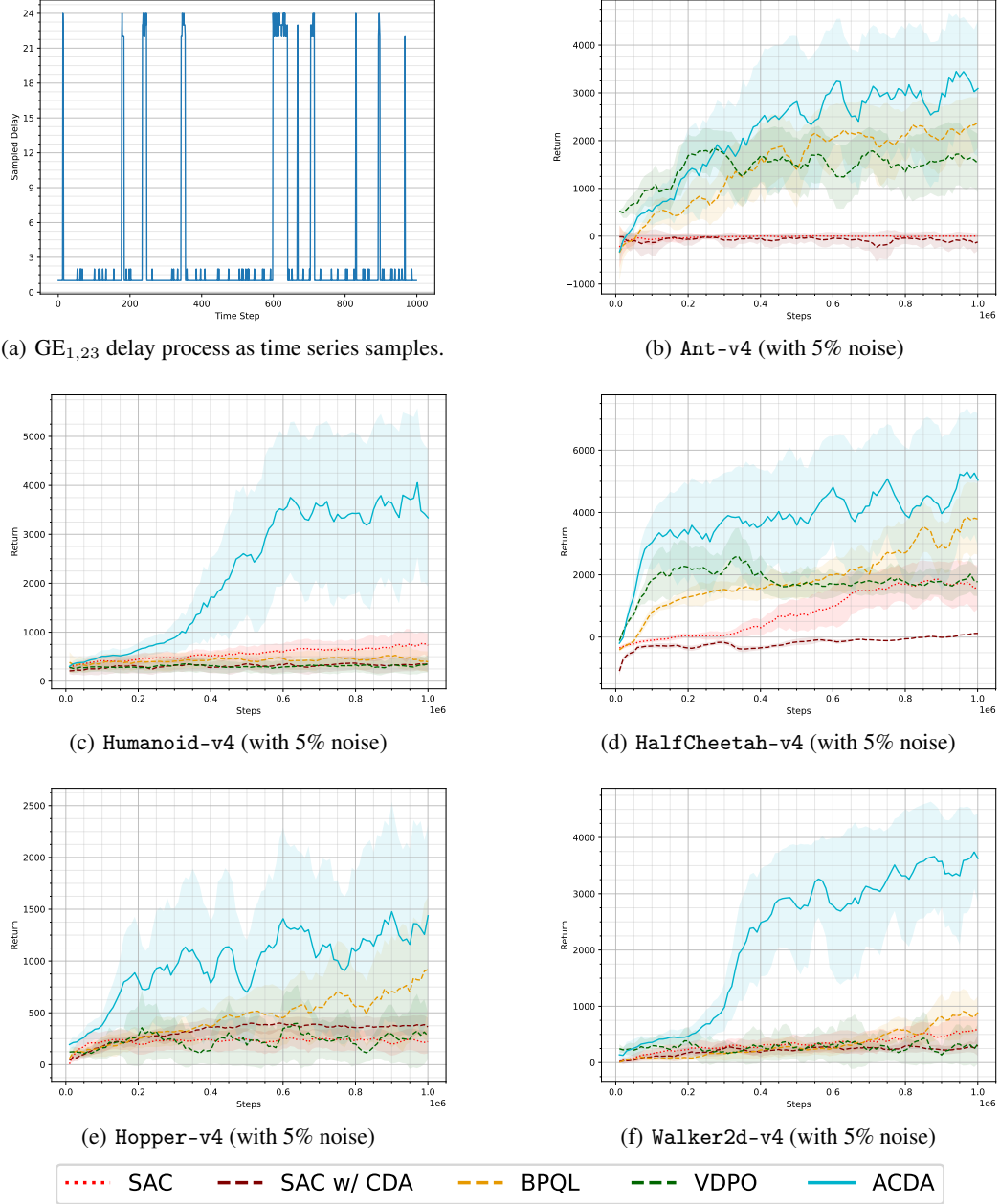


Figure 12: Time series evaluation during training on the $GE_{1,23}$ delay process. All environments have added 5% noise to the actions.

Table 4: Best returns from the $GE_{1,23}$ delay process.

	Ant-v4		Humanoid-v4		HalfCheetah-v4		Hopper-v4		Walker2d-v4	
SAC	14.22 \pm 14.89		862.18 \pm 266.21		2064.18 \pm 223.48		306.91 \pm 51.26		708.33 \pm 221.53	
SAC w/ CDA	69.28 \pm 114.47		414.05 \pm 204.20		128.47 \pm 9.55		426.92 \pm 27.93		428.44 \pm 509.44	
BPQL	2691.88 \pm 129.84		585.19 \pm 163.49		4320.20 \pm 1028.52		1328.71 \pm 937.67		1215.91 \pm 776.93	
VDPO	2163.00 \pm 53.04		417.25 \pm 210.09		3144.23 \pm 1156.52		709.20 \pm 522.01		846.88 \pm 808.67	
ACDA	4112.78 \pm 818.44		4608.76 \pm 1084.52		5984.25 \pm 1885.78		2094.65 \pm 944.20		3863.59 \pm 232.52	

E.1.2 Performance Evaluation under the $GE_{4,32}$ Delay Process

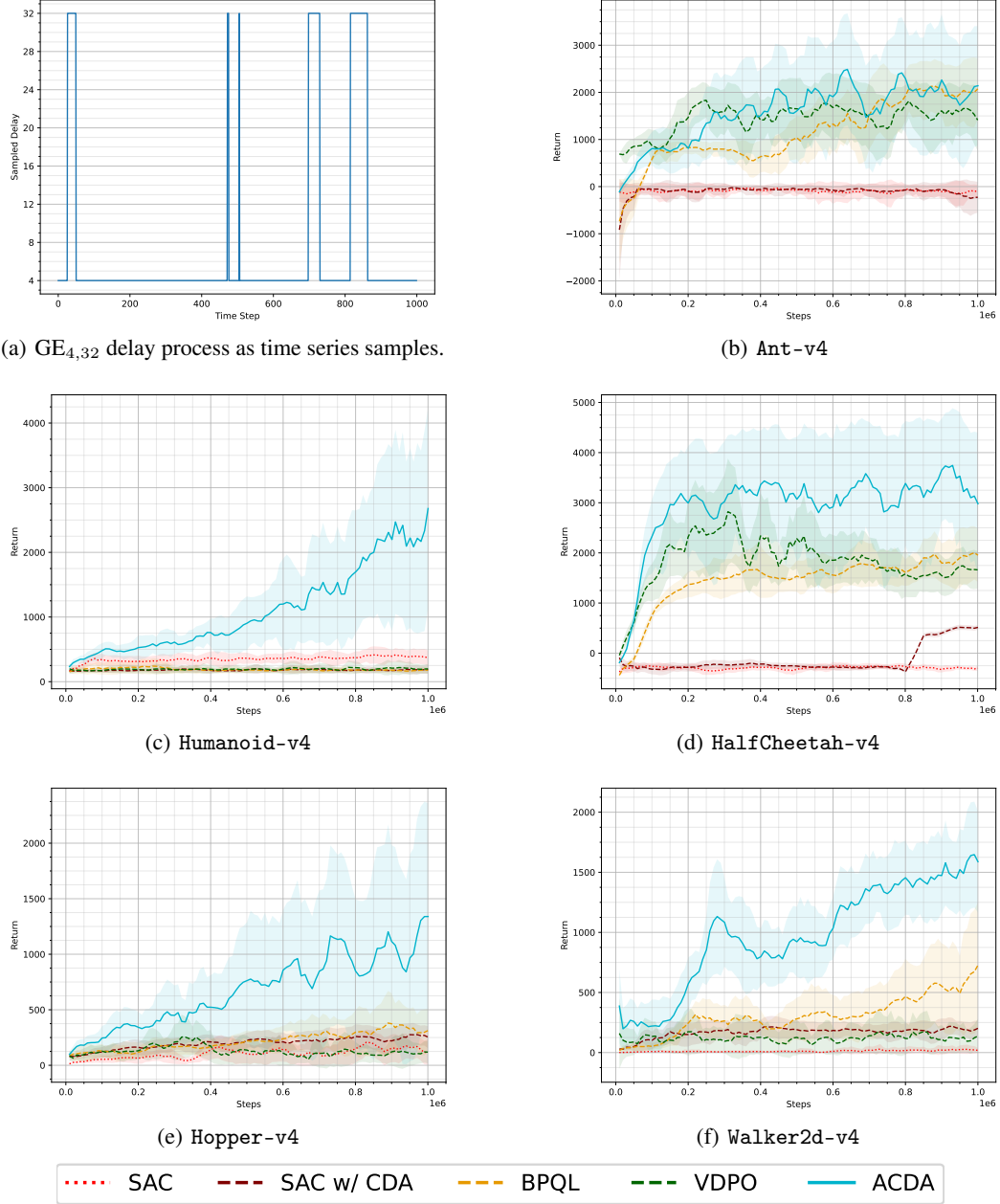


Figure 13: Time series evaluation during training on the $GE_{4,32}$ delay process. All environments have added 5% noise to the actions.

Table 5: Best returns from the $GE_{4,32}$ delay process.

	Ant-v4	Humanoid-v4	HalfCheetah-v4	Hopper-v4	Walker2d-v4
SAC	-5.72 ± 19.62	494.43 ± 156.01	-158.78 ± 65.86	279.74 ± 109.83	60.86 ± 75.59
SAC w/ CDA	18.93 ± 23.64	230.45 ± 99.22	591.32 ± 36.39	315.47 ± 51.49	257.18 ± 73.42
BPQL	2509.52 ± 117.37	276.63 ± 131.70	2136.36 ± 547.04	433.29 ± 381.79	875.09 ± 747.72
VDPO	2266.99 ± 90.89	280.72 ± 169.85	3664.30 ± 929.25	330.44 ± 263.74	344.73 ± 316.82
ACDA	2866.93 ± 1172.46	3725.59 ± 1513.38	4231.15 ± 333.69	1727.79 ± 959.50	1840.58 ± 386.78

E.1.3 Performance Evaluation under the M/M/1 Queue Delay Process

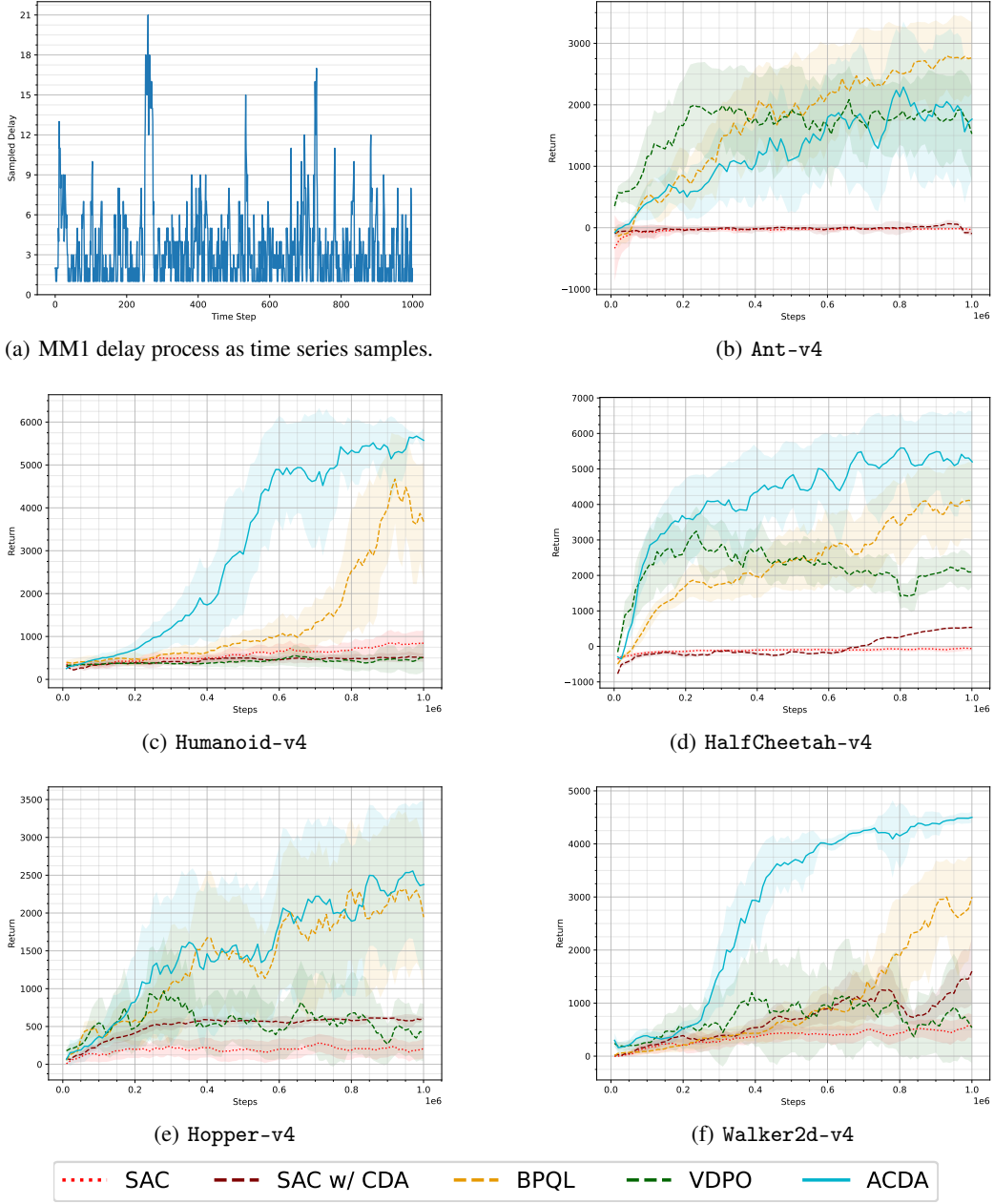


Figure 14: Time series evaluation during training on the MM1 delay process. All environments have added 5% noise to the actions.

Table 6: Best returns from the MM1 delay process.

	Ant-v4	Humanoid-v4	HalfCheetah-v4	Hopper-v4	Walker2d-v4
SAC	-0.58 ± 8.66	921.04 ± 299.47	20.69 ± 94.91	333.06 ± 96.04	604.80 ± 212.37
SAC w/ CDA	102.00 ± 33.77	613.03 ± 157.68	550.84 ± 16.28	627.59 ± 24.62	2005.76 ± 341.30
BPQL	3074.17 ± 106.78	5435.29 ± 68.34	4660.93 ± 448.10	3035.66 ± 103.80	3547.73 ± 133.51
VDPO	2528.67 ± 144.63	720.73 ± 634.35	3831.96 ± 960.07	1459.88 ± 933.11	2144.25 ± 1650.85
ACDA	2898.46 ± 838.07	5805.60 ± 23.04	5898.36 ± 409.10	3122.53 ± 417.37	4562.33 ± 87.98

E.2 Model-Based Distribution Agent vs. Adaptiveness

The purpose of this Appendix is to answer the question whether it is the model-based distribution agent (MDA) or if it is the adaptiveness of ACDA that leads to its high performance. To answer this, we modify the BPQL algorithm to use the MDA policy instead of the direct MLP policy that they used in their original paper.

It is necessary to modify the BPQL algorithm itself since the optimization of the MDA policy is split into two steps with different kind of samples from the replay buffer. If the delay truly was constant, then BPQL with MDA would be the same of the performance of ACDA, due to the perfect conditions for the memorized action selection. However, it is necessary to split these into two algorithms since this cannot capture the M/M/1 queue delay process which cannot be represented as a true constant-delay MDP.

Like Appendix E.1, results are split based on the delay process used. Appendix E.2.1 presents results for the $GE_{1,23}$ delay process, Appendix E.2.2 for the $GE_{4,32}$ delay process, and Appendix E.2.3 for the M/M/1 queue delay process.

These results show that, while BPQL sometimes performs better using the MDA policy, ACDA with its adaptiveness is still the best performing algorithm.

E.2.1 Performance of MDA under the $GE_{1,23}$ Delay Process

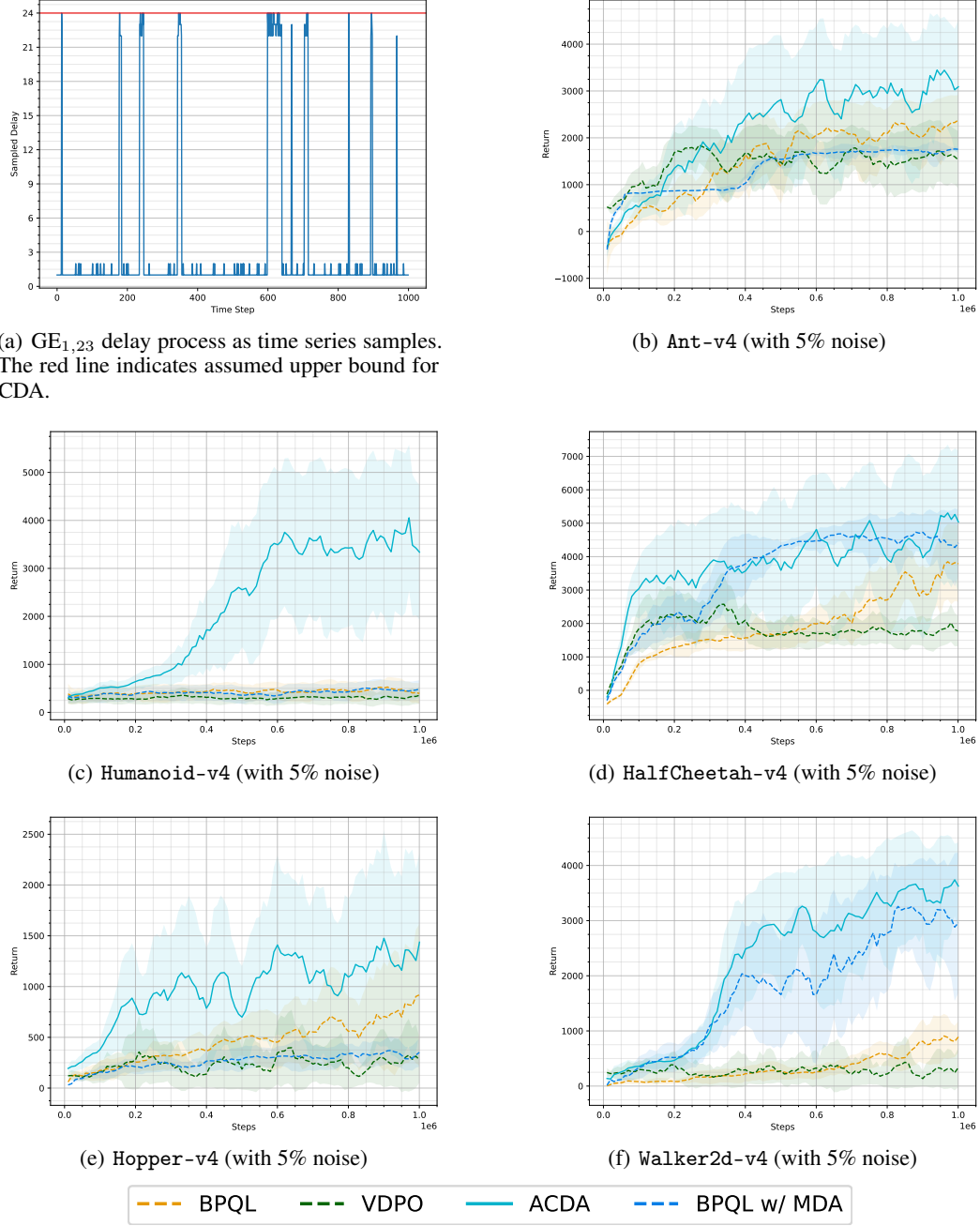
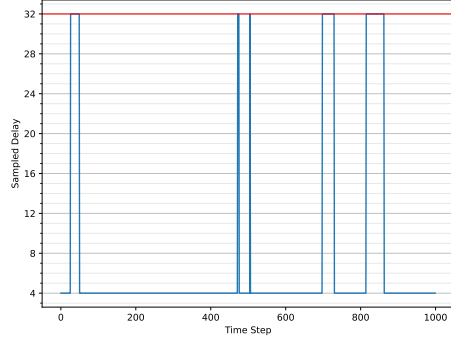


Figure 15: Time series evaluation during training on the $GE_{1,23}$ delay process. All environments have added 5% noise to the actions.

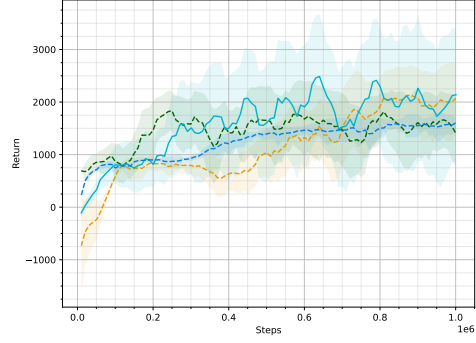
Table 7: Best returns from the $GE_{1,23}$ delay process.

	Ant-v4	Humanoid-v4	HalfCheetah-v4	Hopper-v4	Walker2d-v4
BPQL	2691.88 \pm 129.84	585.19 \pm 163.49	4320.20 \pm 1028.52	1328.71 \pm 937.67	1215.91 \pm 776.93
VDPO	2163.00 \pm 53.04	417.25 \pm 210.09	3144.23 \pm 1156.52	709.20 \pm 522.01	846.88 \pm 808.67
ACDA	4112.78 \pm 818.44	4608.76 \pm 1084.52	5984.25 \pm 1885.78	2094.65 \pm 944.20	3863.59 \pm 232.52
BPQL w/ MDA	1795.29 \pm 23.78	563.36 \pm 96.11	4926.36 \pm 60.08	465.14 \pm 138.86	3681.39 \pm 126.41

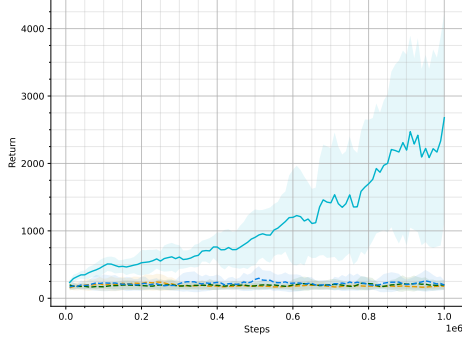
E.2.2 Performance of MDA under the $GE_{4,32}$ Delay Process



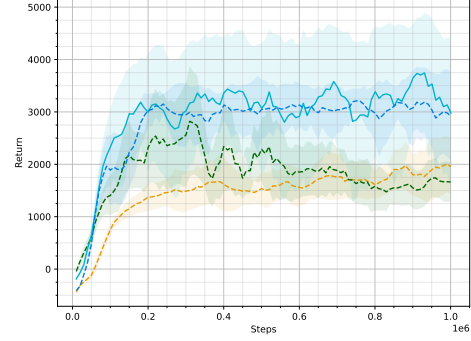
(a) $GE_{4,32}$ delay process as time series samples. The red line indicates assumed upper bound for CDA.



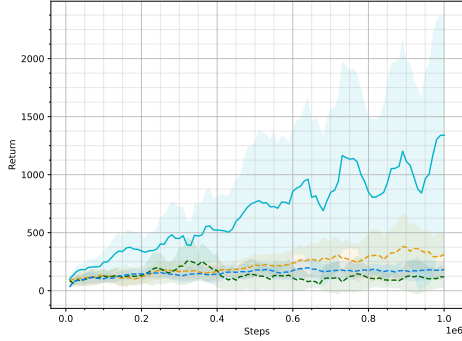
(b) Ant-v4 (with 5% noise)



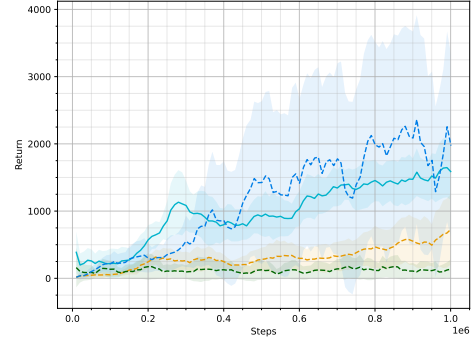
(c) Humanoid-v4 (with 5% noise)



(d) HalfCheetah-v4 (with 5% noise)



(e) Hopper-v4 (with 5% noise)



(f) Walker2d-v4 (with 5% noise)



Figure 16: Time series evaluation during training on the $GE_{4,32}$ delay process. All environments have added 5% noise to the actions.

Table 8: Best returns from the $GE_{4,32}$ delay process.

	Ant-v4	Humanoid-v4	HalfCheetah-v4	Hopper-v4	Walker2d-v4
BPQL	2509.52 \pm 117.37	276.63 \pm 131.70	2136.36 \pm 547.04	433.29 \pm 381.79	875.09 \pm 747.72
VDPO	2266.99 \pm 90.89	280.72 \pm 169.85	3664.30 \pm 929.25	330.44 \pm 263.74	344.73 \pm 316.82
ACDA	2866.93 \pm 1172.46	3725.59 \pm 1513.38	4231.15 \pm 333.69	1727.79 \pm 959.50	1840.58 \pm 386.78
BPQL w/ MDA	1661.41 \pm 43.42	359.46 \pm 156.86	3609.45 \pm 328.37	224.34 \pm 90.12	3015.45 \pm 1428.05

E.2.3 Performance of MDA under the M/M/1 Queue Delay Process

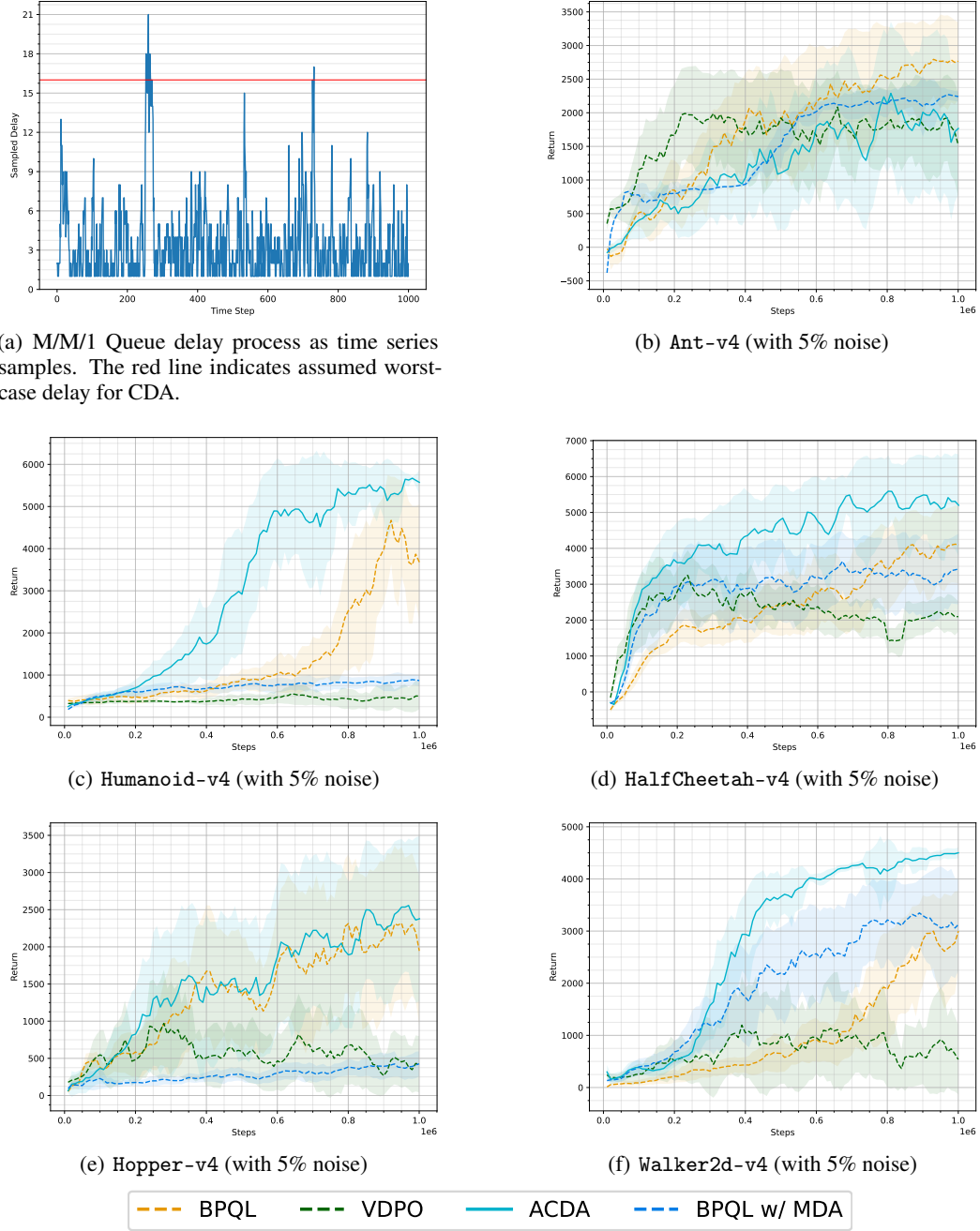


Figure 17: Time series evaluation during training on the MM1 delay process. All environments have added 5% noise to the actions.

Table 9: Best returns from the MM1 delay process.

	Ant-v4	Humanoid-v4	HalfCheetah-v4	Hopper-v4	Walker2d-v4
BPQL	3074.17 \pm 106.78	5435.29 \pm 68.34	4660.93 \pm 448.10	3035.66 \pm 103.80	3547.73 \pm 133.51
VDPO	2528.67 \pm 144.63	720.73 \pm 634.35	3831.96 \pm 960.07	1459.88 \pm 933.11	2144.25 \pm 1650.85
ACDA	2898.46 \pm 838.07	5805.60 \pm 23.04	5898.36 \pm 409.10	3122.53 \pm 417.37	4562.33 \pm 87.98
BPQL w/ MDA	2308.18 \pm 75.13	944.56 \pm 92.79	3953.69 \pm 351.34	512.43 \pm 346.18	3667.61 \pm 142.48

E.3 Results when violating the upper bound assumptions

The $GE_{1,23}$ and $GE_{4,32}$ delay processes occasionally have a very high delay, but most of the time the delay of these are very low. To convert these to a constant-delay MDP, we need to assume the worst-case possible delay of the process. We do this using the CDA method described in Appendix A. CDA can be applied regardless of the constant h that we wish to act under is a worst-case delay or not. Though, CDA only guarantees the MDP property if h is a true upper bound of the delay process.

A natural question is how state-of-the-art approaches performs if we apply CDA to a more favorable constant h , that holds true most of the time and is much lower than the worst-case delay. We answer this by evaluating BPQL and VDPO under more opportunistic constants h . These are compared against the performance of ACDA which can still adapt to much larger delays. We also include an evaluation of BPQL with the MDA policy, as in Appendix E.2, but now when that acts under the opportunistic constant h instead. We present the results of this evaluation in Appendices E.3.1, E.3.2, and E.3.3, which are split based on the delay process used. The opportunistic constant h used is highlighted as a red line in a time series samples plot for each delay process.

The results shows that ACDA still outperforms state-of-the-art in most benchmarks. While BPQL and VDPO can achieve better performance in some cases, ACDA is still performing close to the best algorithm. Also, operating under these opportunistic constants can have significant negative consequences. This is best highlighted by the results in Figure 18(d) where VDPO experiences a collapse in performance under the `HalfCheetah-v4` environment using the $GE_{1,23}$ delay process.

Based on these results, we conclude that the adaptiveness provided by the interaction layer is a necessity to be able to achieve high performance under random unobservable delays. While it is possible to sacrifice the MDP property to gain performance in the constant-delay setting, state-of-the-art still does not outperform the adaptive ACDA algorithm.

E.3.1 $GE_{1,23}$ Delay Process with Low CDA

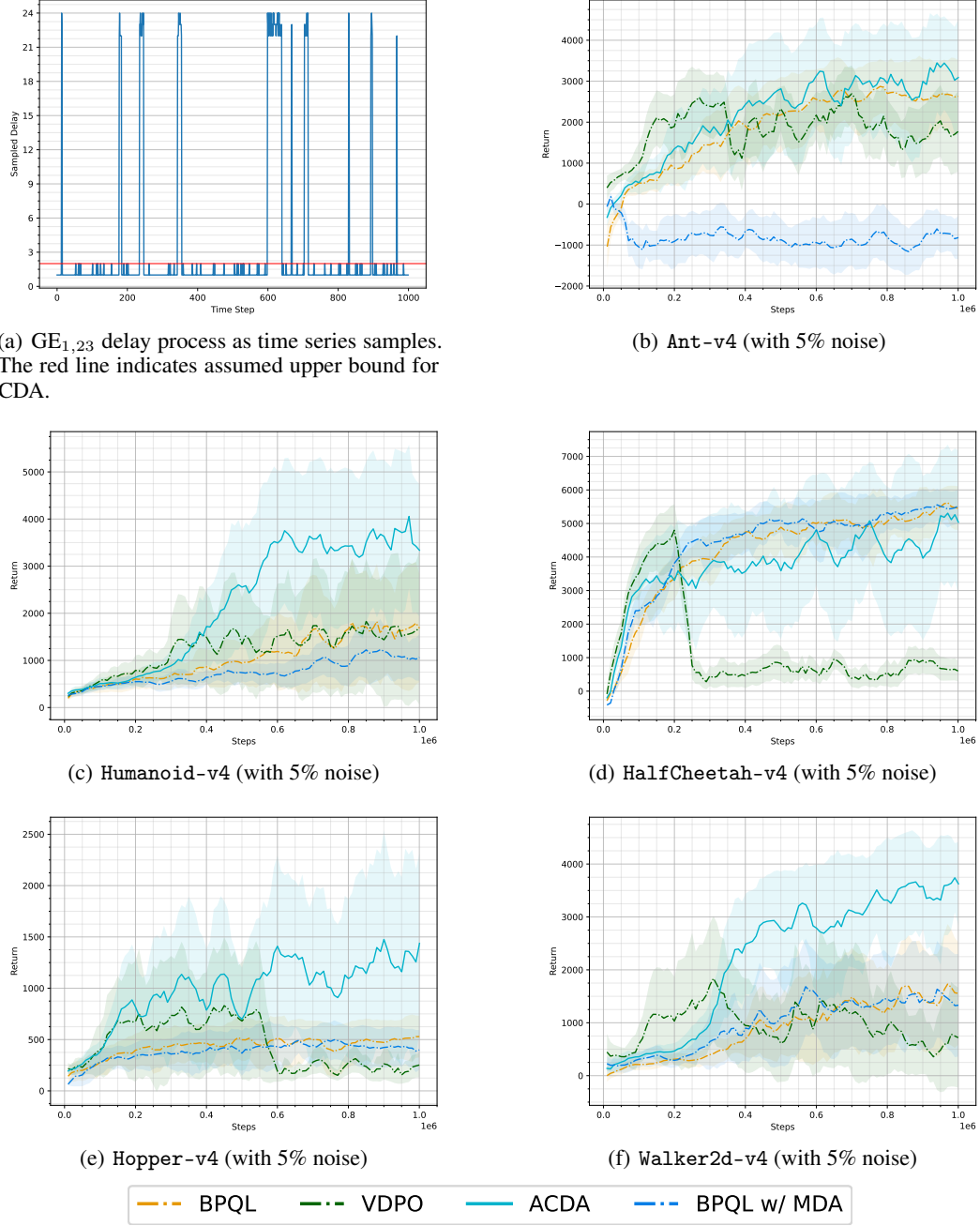
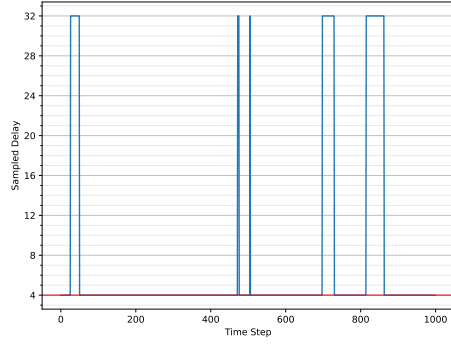


Figure 18: Time series evaluation during training on the $GE_{1,23}$ delay process for opportunistic delay assumptions of $h = 2$ (except for ACDA). All environments have added 5% noise to the actions.

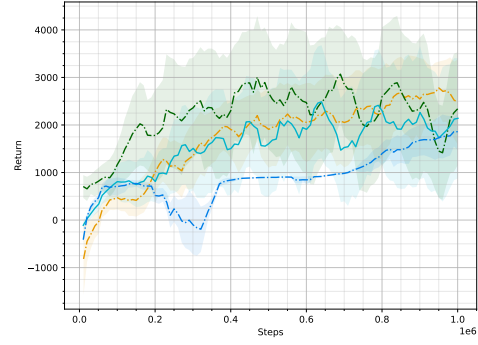
Table 10: Best returns from the $GE_{1,23}$ delay process.

	Ant-v4	Humanoid-v4	HalfCheetah-v4	Hopper-v4	Walker2d-v4
BPQL	3359.65 \pm 288.24	2469.96 \pm 1375.23	5944.67 \pm 395.56	642.54 \pm 420.04	2043.32 \pm 923.00
VDPO	3103.10 \pm 252.19	2658.48 \pm 2044.40	5625.06 \pm 524.23	1113.51 \pm 836.72	2756.73 \pm 1693.64
ACDA	4112.78 \pm 818.44	4608.76 \pm 1084.52	5984.25 \pm 1885.78	2094.65 \pm 944.20	3863.59 \pm 232.52
BPQL w/ MDA	423.46 \pm 73.63	1543.10 \pm 536.14	5710.20 \pm 566.48	545.01 \pm 116.07	1923.28 \pm 838.62

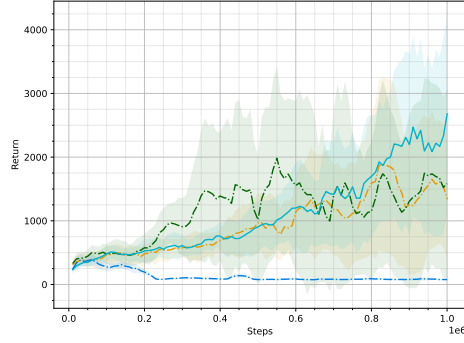
E.3.2 $GE_{4,32}$ Delay Process with Low CDA



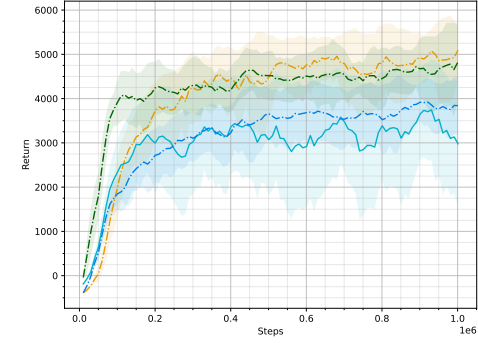
(a) $GE_{4,32}$ delay process as time series samples. The red line indicates assumed upper bound for CDA.



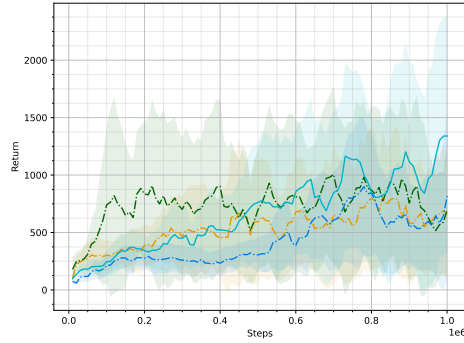
(b) Ant-v4 (with 5% noise)



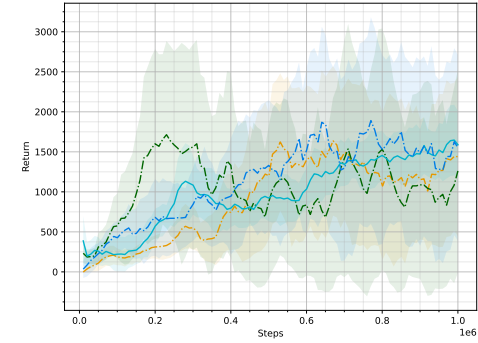
(c) Humanoid-v4 (with 5% noise)



(d) HalfCheetah-v4 (with 5% noise)



(e) Hopper-v4 (with 5% noise)



(f) Walker2d-v4 (with 5% noise)

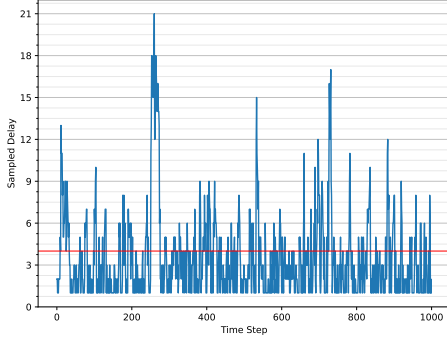


Figure 19: Time series evaluation during training on the $GE_{4,32}$ delay process for opportunistic delay assumptions of $h = 4$ (except for ACDA). All environments have added 5% noise to the actions.

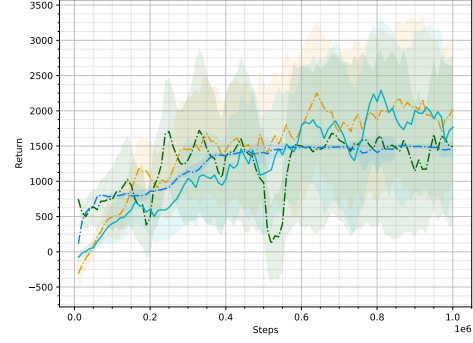
Table 11: Best returns from the $GE_{4,32}$ delay process.

	Ant-v4	Humanoid-v4	HalfCheetah-v4	Hopper-v4	Walker2d-v4
BPQL	3000.00 \pm 754.09	2949.17 \pm 1933.62	5315.27 \pm 559.25	1243.58 \pm 704.53	2107.39 \pm 1219.55
VDPO	3979.56 \pm 331.76	2956.52 \pm 2322.74	5424.96 \pm 306.06	1360.87 \pm 627.11	2234.83 \pm 1776.21
ACDA	2866.93 \pm 1172.46	3725.59 \pm 1513.38	4231.15 \pm 333.69	1727.79 \pm 959.50	1840.58 \pm 386.78
BPQL w/ MDA	2155.47 \pm 84.22	465.58 \pm 82.59	4082.54 \pm 411.47	1312.37 \pm 868.12	2355.23 \pm 1145.73

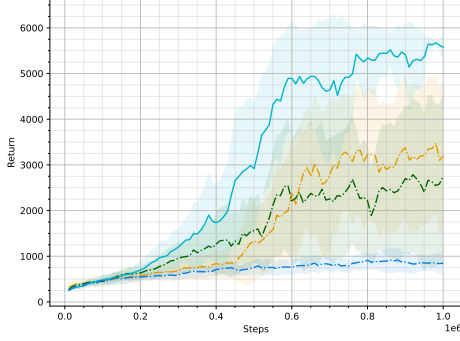
E.3.3 M/M/1 Queue Delay Process with Low CDA



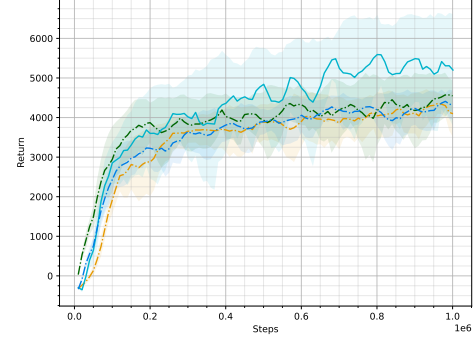
(a) M/M/1 Queue delay process as time series samples. The red line indicates assumed upper bound for CDA.



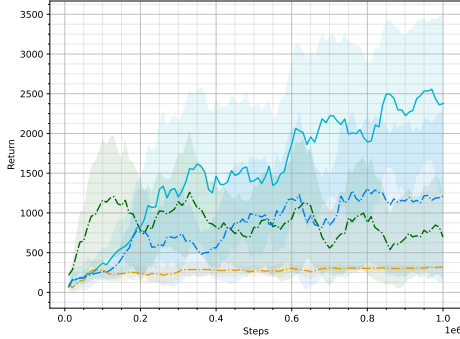
(b) Ant-v4 (with 5% noise)



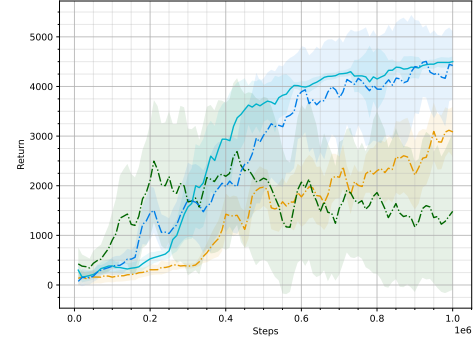
(c) Humanoid-v4 (with 5% noise)



(d) HalfCheetah-v4 (with 5% noise)



(e) Hopper-v4 (with 5% noise)



(f) Walker2d-v4 (with 5% noise)



Figure 20: Time series evaluation during training on the M/M/1 Queue delay process for opportunistic delay assumptions of $h = 4$ (except for ACDA). All environments have added 5% noise to the actions.

Table 12: Best returns from the M/M/1 Queue delay process.

	Ant-v4	Humanoid-v4	HalfCheetah-v4	Hopper-v4	Walker2d-v4
BPQL	2577.34 \pm 1217.11	4158.16 \pm 981.22	4478.64 \pm 193.82	407.91 \pm 179.00	3475.80 \pm 586.89
VDPO	2278.08 \pm 726.85	3349.31 \pm 1668.64	4857.65 \pm 335.88	1628.83 \pm 880.65	3554.77 \pm 1278.22
ACDA	2898.46 \pm 838.07	5805.60 \pm 23.04	5898.36 \pm 409.10	3122.53 \pm 417.37	4562.33 \pm 87.98
BPQL w/ MDA	1541.32 \pm 16.71	1030.55 \pm 185.86	4502.92 \pm 214.25	1665.66 \pm 1210.69	4825.75 \pm 126.28

F Interaction-Delayed Reinforcement Learning with Real-Valued Delay

In Section 3.1 we introduce the delayed MDP using discrete delays measured in steps within the MDP. For real systems described by a MDP, each step corresponds to some amount of real-valued time, possibly controlled by a clock. Any interaction delay with the real system will also correspond to some amount of real-valued time that does not necessarily align with the time taken for a step in the MDP. Therefore it makes sense to talk about delay directly as real-valued time when considering interaction delays for systems in the real world.

In Appendix F.1 we describe the effect that delays have when they are described as real-valued delays. We describe in Appendix F.2 how to implement the interaction layer to handle these real-valued delays.

F.1 Origin and Effect of Delay as Continuous Time

MDPs usually assigns a time t to state, actions, and rewards. This time $t \in \mathbb{N}$ is merely a discrete ordering of events. We model the origin of delays in the real world as elapsed wall clock time in the domain of \mathbb{R}^+ . We use the following notation to distinguish between them:

$$t \in \mathbb{N} \quad (\text{Order of events in MDP.}) \quad (25)$$

$$\tau \in \mathbb{R}^+ \quad (\text{Wall clock time elapsed in the real world.}) \quad (26)$$

In the real world, there is an *interaction delay* in that it takes some time $\tau_{\text{observe}} \in \mathbb{R}^+$ to observe a state, some time $\tau_{\text{decide}} \in \mathbb{R}^+$ to generate the action, and some time $\tau_{\text{apply}} \in \mathbb{R}^+$ to apply the action to the environment. In this time, the state s may evolve independently of an action being applied to the environment. Let this evolution process Δ be defined as

$$\Delta : S \times \mathbb{R}^+ \times S \rightarrow \mathbb{R} \quad (27)$$

$$\text{such that } \tilde{s} \sim \Delta(\cdot | s, \tau) \quad (28)$$

$$\text{subject to } \forall s, \tilde{s}, \tau_1, \tau_2 : \quad \Delta(\tilde{s} | \tilde{s}_i, \tau_2) \Big|_{\tilde{s}_i \sim \Delta(\cdot | s, \tau_1)} = \Delta(\tilde{s} | s, \tau_1 + \tau_2) \quad (29)$$

where $s \in S$ is the state and $\tau, \tau_1, \tau_2 \in \mathbb{R}^+$ is real wall-clock time in which the state has had time to evolve. The evolved state is unknown to the agent and is thus referred to as $\tilde{s} \in S$. The criterion in Equation 29 formally states that it should make no difference whether a state evolved for a single time period or if split into 2 time periods.

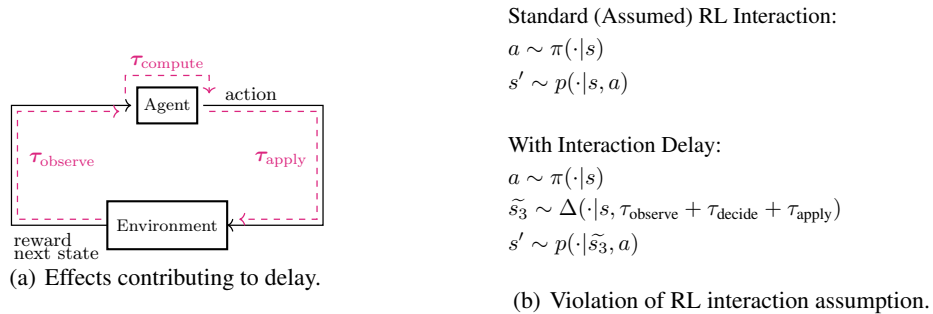


Figure 21: How delays violate the assumption used by state-of-the-art RL algorithms.

If the environment is sufficiently static, like a chess board, then this poses no issue due to that $\Delta(\cdot | s, \tau)$ will always evolve to the same state. If the environment is more dynamic, such as balancing an inverted pendulum, then the interaction delay can result in that state we apply an action to has changed from the state that it was generated from. We illustrate the factors contributing to the

discretize time and ensure that $\tau_{\text{environment}}$ is constant. It operates under the assumptions that the interaction layer can

1. observe the system at any time (read sensors),
2. excite the system at any time (apply actions), and
3. observe and excite with negligible real-world delay (assumed $\tau = 0$).

Under these assumptions, the role of the interaction layer is primarily to

1. maintain an *action buffer* of upcoming actions to apply to the system,
2. accept incoming actions from an agent and insert them into the *action buffer*,
3. ensure that interaction with the system occurs periodically on a fixed interval, and
4. transmit state information back to the agent.

The construction of an interaction layer is realistic for many real-world systems. Using the scenario illustrated in Figure 1 as an example, the interaction layer could be implemented as a microcontroller located on the vehicle itself. We illustrate the interaction layer in Figure 23.

From this perspective the agent acts reactively. The interaction layer manages the interaction with environment, and the agent generated new actions for the action buffer when triggered by emissions from the interaction layer. We denote emitted data from the interaction layer an *observation packet* \mathbf{o}_t , and the data sent to the interaction layer an *action packet* \mathbf{a}_t .